

AD-A131 538

HIGHER ORDER NUMERICAL SIMULATIONS OF THE KNUDSEN LAYER

1/1

(U) AEROSPACE CORP EL SEGUNDO CA VEHICLE ENGINEERING

DIV R L BAKER ET AL 29 APR 83 TR-0083(3729)-2

UNCLASSIFIED

SD-TR-83-47 F04701-82-C-0083

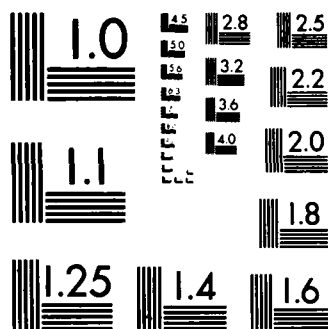
F/G 7/4

NL

END

FILED

14



MICROCOPY RESOLUTION TEST CHART
NATIONAL BUREAU OF STANDARDS-1963-A

(12)

ADA 131538

Higher Order Numerical Simulations of the Knudsen Layer

R. L. BAKER and D. A. NELSON
Vehicle Engineering Division
Engineering Group
The Aerospace Corporation
El Segundo, CA 90245

and

J. S. TURNER
Department of Physics
The University of Texas at Austin
Austin, TX 78712

29 April 1983

Interim Report

APPROVED FOR PUBLIC RELEASE;
DISTRIBUTION UNLIMITED

Prepared for
OFFICE OF NAVAL RESEARCH
Arlington, VA 22217
SPACE DIVISION
AIR FORCE SYSTEMS COMMAND
P.O. Box 92960, Worldway Postal Center
Los Angeles, CA 90009

DTIC
AUG 17 1983
A

DTIC FILE COPY

83 08 16 003

This interim report was prepared for the Office of Naval Research, Arlington, VA 22217, by The Aerospace Corporation, El Segundo, CA 90245, under Contract No. F04701-82-C-0083 with the Space Division, Air Force Systems Command, P.O. Box 92960, Worldway Postal Center, Los Angeles, CA 90009. It was reviewed and approved for The Aerospace Corporation by E.G. Hertler, Director, Aero Engineering Subdivision.

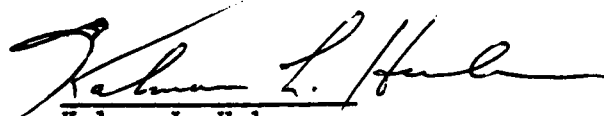
This report has been reviewed by the Public Affairs Office (PAS) and is releasable to the National Technical Information Service (NTIS). At NTIS, it will be available to the general public, including foreign nations.

This technical report has been reviewed and is approved for publication. Publication of this report does not constitute Air Force approval of the report's findings or conclusions. It is published only for the exchange and stimulation of ideas.



Gerhard E. Aichinger
Technical Advisor

FOR THE COMMANDER



Kalman L. Huler
Chief, Special Contracts Office

UNCLASSIFIED

SECURITY CLASSIFICATION OF THIS PAGE (When Data Entered)

REPORT DOCUMENTATION PAGE		READ INSTRUCTIONS BEFORE COMPLETING FORM
1. REPORT NUMBER SD-TR-83- 47	2. GOVT ACCESSION NO. AD-A131 538	3. RECIPIENT'S CATALOG NUMBER
4. TITLE (and Subtitle) HIGHER ORDER NUMERICAL SIMULATIONS OF THE KNUDSEN LAYER		5. TYPE OF REPORT & PERIOD COVERED Interim Report 1 Oct. 1981 - 30 Sept. 1982
7. AUTHOR(s) R. L. Baker & D. A. Nelson (The Aerospace Corp.) J. S. Turner (University of Texas at Austin)		6. PERFORMING ORG. REPORT NUMBER TR-0083(3729)-2
9. PERFORMING ORGANIZATION NAME AND ADDRESS The Aerospace Corporation El Segundo, California 90245		8. CONTRACT OR GRANT NUMBER(s) F04701-82-C-0083
11. CONTROLLING OFFICE NAME AND ADDRESS Office of Naval Research Eastern/Central Regional Office Boston, MA 02210		10. PROGRAM ELEMENT, PROJECT, TASK AREA & WORK UNIT NUMBERS
14. MONITORING AGENCY NAME & ADDRESS (if different from Controlling Office) Space Division Air Force Systems Command Los Angeles, CA 90009		12. REPORT DATE 29 April 1983
		13. NUMBER OF PAGES 57
		15. SECURITY CLASS. (of this report) Unclassified
		15a. DECLASSIFICATION/DOWNGRADING SCHEDULE
16. DISTRIBUTION STATEMENT (of this Report) Approved for public release; distribution unlimited		
17. DISTRIBUTION STATEMENT (of the abstract entered in Block 20, if different from Report)		
18. SUPPLEMENTARY NOTES		
19. KEY WORDS (Continue on reverse side if necessary and identify by block number) Knudsen layer Boltzmann equation Molecular Dynamics Nonequilibrium phase change Monte Carlo simulation Carbon vaporization kinetics Carbon vapor pressure Nonequilibrium thermodynamics Strong evaporation processes Laser vaporization		
20. ABSTRACT (Continue on reverse side if necessary and identify by block number) The infinitesimal nonequilibrium region (Knudsen layer) that occurs at phase interfaces when there is net mass transfer, has been theoretically investigated for the case of strong evaporation. The rate of collisional relaxation processes in the layer, which determines the net transfer of mass, momentum, and energy across the layer, has been studied using models at three levels of mathematical complexity (completeness).		

DD FORM 1473
(FACSIMILE)

UNCLASSIFIED

SECURITY CLASSIFICATION OF THIS PAGE (When Data Entered)

UNCLASSIFIED

SECURITY CLASSIFICATION OF THIS PAGE (When Data Entered)

19. KEY WORDS (Continued)

20. ABSTRACT (Continued)

↓

Calculated results obtained by Monte Carlo direct simulation of the Boltzmann equation and, by the method of Molecular Dynamics, have been compared with approximate solutions based upon the nonlinear mass, momentum, and energy conservation equations. The comparisons indicate the validity of the approximate method in predicting the essential features of the Knudsen layer region, i.e., the net mass transfer rate and the static pressure jump across the layer, for both single and multiple species cases. We are interested in the multispecies case for the interpretation of laser-vaporized carbon ablation data to obtain vapor pressure and vaporization kinetics information. Further use of the higher order solution methods is anticipated to investigate theoretically difficult physical/chemical problems such as the effect of thermal fluctuations in nonlinear chemically reacting systems.

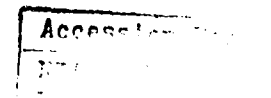
A

UNCLASSIFIED

SECURITY CLASSIFICATION OF THIS PAGE (When Data Entered)

PREFACE

This work was supported by the Office of Naval Research under Air Force/Space Division Contract No. F04701-81-C-0082. The continuing support and encouragement of contract monitor Dr. L. H. Peebles, Jr. is gratefully acknowledged. ♣



A

CONTENTS

I.	INTRODUCTION.....	7
II.	MOMENT EQUATION SOLUTIONS.....	11
	A. Single Species Solutions.....	11
	1. Full Moment Equation Approach.....	11
	2. Simplified Moment Equation Approach of Cong and Bird....	15
	B. Multispecies Vaporization.....	16
III.	MONTE CARLO SIMULATION OF THE BOLTZMANN EQUATION.....	19
	A. Higher Order Methods.....	19
	B. Description of Monte Carlo/Boltzmann Equation Simulation Method.....	20
	C. Application to the Knudsen Layer.....	22
	1. Computer Program Development.....	22
	2. Downstream Boundary Condition.....	23
	3. Simulation of the "Flat Sink" Boundary Condition.....	24
	4. Calculation Time Steps and Collision Dynamics.....	25
IV.	MOLECULAR DYNAMICS SIMULATIONS.....	29
	A. Description of Method.....	29
	B. Application to the Knudsen Layer Problem.....	30
V.	COMPARISON OF CALCULATED RESULTS.....	37
	A. Single Species Solutions, Three-Dimensional Molecular Collisions.....	37
	B. Single Species Solutions, Two-Dimensional Molecular Collisions.....	41
	C. Multispecies Solutions.....	47
VI.	OTHER APPLICATIONS.....	51
VII.	SUMMARY AND CONCLUSIONS.....	55
	REFERENCES.....	57
	APPENDICES:	
	A. SOURCE BOUNDARY CONDITIONS.....	A-1
	B. TRANSLATIONAL ENERGY FLUX EQUATION FOR TWO-DIMENSIONAL MOLECULAR COLLISIONS.....	B-1

FIGURES

1.	Macroscopic Property Changes Across Knudsen Layer.....	12
2.	Main Computational Procedures of the Direct Simulation Monte Carlo Method.....	21
3.	Cell Grid for Knudsen Layer Simulation.....	26
4.	The Three Area Method.....	32
5.	Periodic Boundary Conditions for Areas 1 and 3.....	33
6.	Boundary Conditions for Area 2 Simulating the Knudsen Layer.....	35
7.	Number of Particles in Area 2 versus Number of Collisions.....	36
8.	Comparison of Predicted Mass Loss and Pressure Ratios.....	39
9.	Knudsen Layer Profiles, $M_{\text{edge}} = 0.58$	42
10.	Knudsen Layer Profiles, $M_{\text{edge}} = 1.0$	43
11.	Comparison of Calculated Results Obtained from Different Solution Methods, Two-Dimensional Collisions.....	44
12.	Moment Equation Solutions for Knudsen Layer Jump Conditions.....	45
13.	Parameter A^2/B as a Function of Knudsen Layer Edge Mach Number.....	46
14.	Thermodynamic Temperature Probe Experiment.....	52

TABLES

1.	Collision Dynamics Parameters.....	27
2.	Predicted Ratios: Single Species.....	40
3.	Predicted Ratios: Single Species and Multispecies.....	49
4.	Predicted Species Distributions.....	50

I. INTRODUCTION

Whenever a net transfer of mass occurs across a phase interface, an infinitesimal nonequilibrium region exists at the interface. Across this region the transferring substance "relaxes" from one state to another with an accompanying transfer of momentum and energy. The thickness of this layer is the order of a few mean free paths, and it has come to be generally referred to as the Knudsen layer.¹ Knudsen layers are of theoretical interest for at least two important reasons. The rate of relaxation processes occurring in the Knudsen layer determines both the net transfer of mass, momentum, and energy across the layer and the boundary conditions for relaxation processes outside the layer.

An adequate theoretical understanding of Knudsen layer processes is thus needed to specify external boundary conditions, accurately predict interphase transfer rates, and potentially use such predictions as a diagnostic tool. For instance, we have recently utilized a Knudsen layer model to obtain carbon vapor pressure and vaporization kinetics information from laser-vaporized carbon ablation data.^{2,3} It may be possible to obtain internal degrees of freedom (rotational, vibrational) as well as chemical relaxation rate information from a detailed Knudsen layer analysis of such data.

¹Knudsen, M., Ann. Phys. (Leipzig), 47, 1915, pp. 697-708.

²Baker, R.L., "Carbon Nonequilibrium Phase Change," Office of Naval Research Interim Report, TR-0081(6728-02)-1, The Aerospace Corporation, El Segundo, CA, Dec. 1981.

³Baker, R.L. and M.A. Covington, "The High Temperature Thermochemical Properties of Carbon," Office of Naval Research Interim Report, TR-0082(2729)-1, The Aerospace Corporation, El Segundo, CA, Mar. 1982.

Most Knudsen layer analyses conducted by early investigators neglected the momentum equation, and sometimes the energy equation, and retained only linear terms. An excellent summary of approaches utilizing linearized equations is given by Weichert.⁴ Baker⁵ adapted one of the linearized models, which utilized a nonequilibrium thermodynamics approach,⁶ to the carbon phase change system by assuming that carbon vapor is made up of species C_3 molecules only. The same approach was later extended to consider the actual multiple species (multispecies) character of carbon vapor.⁷

More recently, the desire to theoretically describe intensive or "strong" evaporation processes, such as the evaporation of metal vapor into a vacuum by laser irradiation, has led to the development of Knudsen layer models that retain all the nonlinear terms in the mass, momentum, and energy conservation equations.⁸⁻¹⁰ Adaptation and extension of these models to the carbon single species² and multispecies³ cases have also been completed. We used the Ref. 3 model to obtain carbon vapor pressure and vaporization kinetics information from carbon laser ablation data.

⁴Weichert, H., "Boundary Conditions for the Liquid-Vapor Interface of Helium II," J. Phys. C: Solid State Physics, 9, 1976, pp. 553-569.

⁵Baker, R.L., "An Irreversible Thermodynamics Model for Graphite Sublimation in Radiation Environments," Progress in Astronautics and Aeronautics: Outer Planet Heating and Thermal Protection Systems, 64, R. Viskanta (ed.), AIAA, New York, 1979, pp. 210-227.

⁶Bornhorst, W.J. and G.N. Hatsopoulos, "Analysis of a Phase Change by the Methods of Irreversible Thermodynamics," J. Appl. Mech., 34, Dec. 1967, pp. 840-846.

⁷Baker, R.L., "A Multiple Species Nonequilibrium Thermodynamics Model for Carbon Sublimation," J. Nonequil. Thermo., 7(5), 1982, pp 309-322.

⁸Anisimov, S.I., "Vaporization of Metal Absorbing Laser Radiation," Sov. Phys. JETP, 27(1), 1968, pp. 182-183.

⁹Ytrehus, T., "Theory and Experiments on Gas Kinetics in Evaporation," Progress in Astronautics and Aeronautics: Rarefied Gas Dynamics, 51 (II), J.L. Potter (ed.), AIAA, New York, 1977, pp. 1197-1212.

¹⁰Knight, C.J., "Theoretical Modeling of Rapid Surface Vaporization with Back-Pressure," AIAA J., 17, May 1979, pp. 519-523.

The analyses of Refs. 2, 3, and 8 through 10 are based upon the full nonlinear equations for the conservation of mass, momentum, and energy across the Knudsen layer, i.e., on three moment equations. However, as discussed in Section II of this report, ad hoc closure assumptions are necessary in order to obtain a solution to the three moment equations. Thus, the present work on "higher order" solutions to the Knudsen layer problem was motivated by the desire to eliminate the need for any arbitrary closure and to determine the accuracy of the moment equation solutions by comparing them with the higher order solutions.

The higher order approaches which have been considered are a Monte Carlo simulation method for obtaining solutions to the Boltzmann equation¹¹ and the Method of Molecular Dynamics.¹² We have applied both approaches to the Knudsen layer problem and obtained calculated results. Boltzmann equation solutions have been obtained for both the single species and the multispecies evaporation problems. Because of the complexity associated with following the movement of every molecule, Molecular Dynamics solutions have been obtained only for single species evaporation and two-dimensional molecular collisions. Three-moment equation and Monte Carlo/Boltzmann equation solutions were also obtained for the two-dimensional molecular collisions case, and this made a comparison of all three methods possible.

Sections II through IV discuss moment equation, Boltzmann equation, and Molecular Dynamics solutions of the Knudsen layer problem, respectively. In Section V, calculated results from all three methods are compared and the adequacy of moment equation solutions is discussed. Section VI briefly describes some additional potential applications of our higher order Knudsen layer solution approaches. A summary of results and conclusions is given in Section VII.

¹¹Bird, G.A., Molecular Gas Dynamics, Oxford University Press, London, 1976.

¹²Hansen, H.W., and W.C. Schieve, J. Stat. Phys., 3, 1971, p. 35.

II. MOMENT EQUATION SOLUTIONS

The purpose of the following discussion is to review earlier Knudsen layer work that has been carried out using the moment equation approach for both single species and multispecies cases. In addition, new work in which the single species analytic solutions are extended to the case of two-dimensional, instead of three-dimensional molecular collisions is also presented. The following discussion emphasizes the necessity of making additional, somewhat arbitrary, "ad hoc" assumptions in order to obtain a solution to the moment equations. The higher order solutions discussed in Sections III and IV were motivated by the desire to obtain solutions without these arbitrary assumptions and to compare them with the moment equation solution.

A. SINGLE SPECIES SOLUTIONS

1. Full Moment Equation Approach

A schematic representation of a Knudsen layer is shown in Fig. 1. The objective is to express the Knudsen layer edge values of pressure p , density ρ , temperature T , and velocity u in terms of the saturated vapor values at the solid-vapor interface p_s , ρ_s , and T_s and the mass throughput, $\dot{m} = \rho u$. Instead of \dot{m} , the independent variable is usually considered to be the Mach number $M = u/\sqrt{\gamma RT}$. The quantities \dot{m} and M are related by

$$\dot{m} = \rho u = \sqrt{\frac{\gamma \mathcal{M}}{RT}} p M \quad (1)$$

where γ is the ratio of specific heats, \mathcal{M} is the molecular weight, and R is the gas constant.

Following the approach of Anisimov,⁸ the equations for the conservation of mass, momentum, and energy across the Knudsen layer for a monatomic gas may be written as

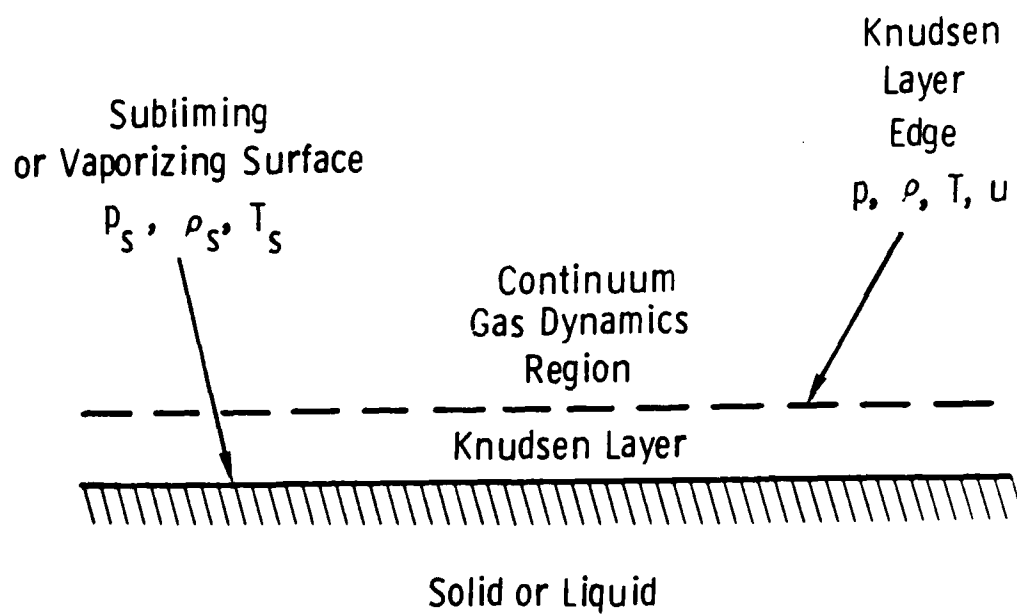


Fig. 1. Macroscopic Property Changes Across Knudsen Layer

$$\rho u = \alpha_v \rho_s \sqrt{\frac{RT_s}{2\pi}} + \alpha_c \beta \rho \sqrt{\frac{RT}{2\pi}} \left[\sqrt{\pi} m \operatorname{erfc}(m) - e^{-m^2} \right] \quad (2)$$

$$\rho u^2 + \rho RT = \frac{\alpha_v}{2} \rho_s RT_s + (2 - \alpha_c) \beta \rho RT \left[(m^2 + 1/2) \operatorname{erfc}(m) - \frac{m}{\sqrt{\pi}} e^{-m^2} \right] \quad (3)$$

$$\begin{aligned} \rho u \left(\frac{5}{2} RT + \frac{1}{2} u^2 \right) &= \alpha_v \rho_s \sqrt{\frac{RT_s}{2\pi}} [2RT_s] \\ &+ \alpha_c \beta \rho RT \sqrt{\frac{RT}{2\pi}} \left[m \left(m^2 + \frac{5}{2} \right) \sqrt{\pi} \operatorname{erfc}(m) - (m^2 + 2) e^{-m^2} \right] \end{aligned} \quad (4a)$$

The terms containing β on the right-hand sides of these equations arise from the backscattered molecules which collide with the vaporizing surface. The velocity distribution function for these molecules is not known. However, the density, temperature, and mean velocity from this distribution function are needed to define the right-hand side terms. Anisimov defined the density as $\beta \rho$ and then somewhat arbitrarily assumed the temperature to be the Knudsen layer edge temperature T and the velocity to be the Knudsen layer edge velocity u .

With these assumptions, Eqs. (2) through (4) are obtained and form a closed set which can be solved for β , ρ/ρ_s and T/T_s as a function of the speed ratio $m = u/\sqrt{2RT}$. However, the effect of the arbitrary assumptions on the accuracy of the solutions is not known.

In the above equations, α_v is the vaporization coefficient and α_c is the condensation coefficient. Anisimov further assumed $\alpha_v = \alpha_c = 1.0$ and $\gamma = 5/3$. Analytic solutions for the case of $\alpha_v \neq \alpha_c \neq 1$ and arbitrary values of γ are discussed in Ref. 2. For present purposes, it is sufficient to consider the simpler case of $\alpha_v = \alpha_c = 1.0$. If the molecular collisions all occur in a plane,

i.e., two-dimensional collisions, then Eq. (4a) becomes

$$\begin{aligned} \rho u \left(2RT + \frac{1}{2} u^2 \right) &= \alpha_v \rho_s \sqrt{\frac{R}{2\pi}} \left[\frac{3}{2} RT_s \right] \\ &+ \alpha_c \beta \rho RT \sqrt{\frac{RT}{2\pi}} \left[m(m^2 + 2) \sqrt{\pi} \operatorname{erfc}(m) - \left(m^2 + \frac{3}{2} \right) e^{-m^2} \right] \end{aligned} \quad (4b)$$

The derivation of this equation is given in Appendix A.

When Eqs. (2), (3), and (4a) are combined, the following expressions for β , T/T_s , and ρ/ρ_s as a function of m are obtained.

$$\beta = \left\{ (2m^2 + 1) - m\pi^{1/2} \left(\frac{T_s}{T} \right)^{1/2} \right\} \frac{\rho_s}{\rho} \left(\frac{T_s}{T} \right)^{1/2} e^{m^2} \quad (5)$$

$$\frac{T}{T_s} = \left[-\frac{m\pi^{1/2}}{8} + \sqrt{\frac{m^2\pi}{64} + 1} \right]^2 \quad (6a)$$

$$\begin{aligned} \frac{\rho}{\rho_s} &= \left[(m^2 + \frac{1}{2}) \operatorname{erfc}(m) e^{m^2} - m\pi^{-1/2} \right] \left[-\frac{m\pi^{1/2}}{8} + \sqrt{\frac{m^2\pi}{64} + 1} \right]^{-1} \\ &+ \frac{1}{2} \left[1 - \pi^{1/2} m \operatorname{erfc}(m) e^{m^2} \right] \left[-\frac{m\pi^{1/2}}{8} + \sqrt{\frac{m^2\pi}{64} + 1} \right]^{-2} \end{aligned} \quad (7a)$$

For two-dimensional molecular collisions, Eq. (5) remains the same, and Eqs. (6a) and (7a) are replaced by

$$\frac{T}{T_s} = \left[-\frac{m\pi^{1/2}}{6} + \sqrt{\frac{m^2\pi}{36} + 1} \right]^2 \quad (6b)$$

$$\begin{aligned} \frac{\rho}{\rho_s} &= \left[(m^2 + \frac{1}{2}) \operatorname{erfc}(m) e^{m^2} - m\pi^{-1/2} \right] \left[-\frac{m\pi^{1/2}}{6} + \sqrt{\frac{m^2\pi}{36} + 1} \right]^{-1} \\ &+ \frac{1}{2} \left[1 - \pi^{1/2} m \operatorname{erfc}(m) e^{m^2} \right] \left[-\frac{m\pi^{1/2}}{6} + \sqrt{\frac{m^2\pi}{36} + 1} \right]^{-2} \end{aligned} \quad (7b)$$

2. Simplified Moment Equation Approach of Cong and Bird

If the condensation coefficient α_c is assumed to be zero, then the moment equations are considerably simplified. The mass conservation equation becomes simply

$$\rho u = \rho_s \sqrt{\frac{RT_s}{2\pi}} \quad (8)$$

Following Cong and Bird,¹³ the right-hand sides of the momentum and energy equations are simplified by introducing factors A and B, i.e.

$$\rho u^2 + \rho RT = \frac{1}{2} A \rho_s RT_s \quad (9)$$

$$\rho u \left[\frac{5}{2} RT + \frac{1}{2} u^2 \right] = \left[\frac{2}{\pi} \right]^{1/2} B \rho_s (RT_s)^{3/2} \quad (10a)$$

For planar molecular collisions (See Appendix A), Eq. (10a) becomes

$$\rho u \left[2RT + \frac{1}{2} u^2 \right] = \left[\frac{3}{2\pi} \right]^{1/2} B \rho_s (RT_s)^{3/2} \quad (10b)$$

For two-dimensional molecular collisions, the ratio of specific heats γ for a monatomic gas can be shown as 2 instead of the 5/3 value for three-dimensional molecular collisions. This occurs because, in the two-dimensional collision case, the translational energy is RT instead of the normal $(3/2)RT$. When the Mach number is consistently defined with these values of γ , the following solutions to the above equations are obtained:

For three-dimensional molecular collisions

$$\frac{T_s}{T} = \frac{5}{4B} \left[1 + \frac{1}{3} M^2 \right] \quad (11a)$$

$$\frac{\rho_s}{\rho} = \left(\frac{10\pi}{3} \right)^{1/2} \left(\frac{T_s}{T} \right)^{-1/2} M \quad (11b)$$

$$\frac{A^2}{B} = \left(\frac{24}{25\pi} \right) \left\{ \frac{\left[1 + \frac{5}{3} M^2 \right]^2}{\left[1 + \frac{1}{3} M^2 \right] M^2} \right\} \quad (11c)$$

¹³Cong, T.T. and G.A. Bird, "One-Dimensional Outgassing Problem," Phys. Fluids, 21(3), 1978, pp. 327-333.

and for two-dimensional molecular collisions

$$\frac{T_s}{T} = \frac{4}{3B} \left[1 + \frac{1}{2} M^2 \right] \quad (12a)$$

$$\frac{\rho_s}{\rho} = (4\pi)^{1/2} \left(\frac{T_s}{T} \right)^{-1/2} M \quad (12b)$$

$$\frac{A^2}{B} = \frac{3}{4\pi} \left\{ \frac{\left[1 + 2M^2 \right]^2}{\left[1 + \frac{1}{2} M^2 \right] M^2} \right\} \quad (12c)$$

B. MULTISPECIES VAPORIZATION

For n species, the conservation equations across the Knudsen layer are^{3,11}

$$[\rho_i u_i]_J = \left[\alpha_{v_i} \rho_{s_i} \sqrt{\frac{RT_s}{2\pi \mathcal{M}_i}} \right]_{J_s} + \left[\alpha_{c_i} \bar{\rho}_{b_i} \bar{T}_b^{1/2} \rho_i \sqrt{\frac{RT}{2\pi \mathcal{M}_i}} f^1(x_i) \right]_{J_b} \quad (13)$$

($i = 1, 2, \dots, n$)

$$\left[\rho \left(u^2 + \frac{RT}{\mathcal{M}} \right) \right]_J = \left[\frac{RT_s}{2} \sum_{i=1}^n \frac{\alpha_{v_i} \rho_{s_i}}{\mathcal{M}_i} \right]_{J_s} + \left[\bar{T}_b RT \sum_{i=1}^n \rho_{b_i} (2 - \alpha_{c_i}) \frac{\rho_i}{\mathcal{M}_i} f^2(x_i) \right]_{J_b} \quad (14)$$

$$\left\{ \rho u \left[\left(\frac{5}{2} + G \right) \frac{RT}{\mathcal{M}} + \frac{1}{2} u^2 \right] \right\}_J = \left[\frac{(RT_s)^{3/2}}{(2\pi)^{1/2}} \sum_{i=1}^n \frac{\alpha_{v_i} \rho_{s_i}}{\mathcal{M}_i^{3/2}} (2 + G_i) \right]_{J_s} + \left\{ \bar{T}_b^{3/2} \frac{(RT)^{3/2}}{(2\pi)^{1/2}} \sum_{i=1}^n \frac{\alpha_{c_i} \bar{\rho}_{b_i} \rho_i}{\mathcal{M}_i^{3/2}} \left[f^3(x_i) + f^1(x_i) G_i \right] \right\}_{J_b} \quad (15)$$

The functions $f(x_i)$ are given by

$$f^1(x_i) = \pi^{1/2} x_i \operatorname{erfc}(x_i) - e^{-x_i^2} \quad (16a)$$

$$f^2(x_i) = \left(x_i^2 + \frac{1}{2}\right) \operatorname{erfc}(x_i) - \frac{x_i}{\pi^{1/2}} e^{-x_i^2} \quad (16b)$$

$$f^3(x_i) = x_i \left(x_i^2 + \frac{5}{2}\right) \pi^{1/2} \operatorname{erfc}(x_i) - (x_i^2 + 2) e^{-x_i^2} \quad (16c)$$

where

$$x_i = \bar{w}_i \bar{T}_b \frac{u_i}{\sqrt{2RT/M_i}} \quad (16d)$$

Quantities not yet defined in the above equations are the convective velocity w of the backscattered molecules striking the surface and G , which is related to the ratio of specific heats γ by

$$G(\gamma) = \frac{(5 - 3\gamma)}{2(\gamma - 1)} \quad (17)$$

The quantities in Eqs. (13) through (16) are dimensional except for x_i , \bar{T}_b , and \bar{w}_i . The latter two variables are nondimensionalized by T and u , respectively, and x_i is directly proportional to a species Mach number M_i , i.e.

$$\bar{T}_b = T_b/T \quad (18a)$$

$$\bar{w}_i = w_i/u \quad (18b)$$

$$x_i = \sqrt{\gamma_i/2} \bar{w}_i \bar{T}_b M_i \quad (18c)$$

In the process of obtaining the single species equations, (2) through (4), the "ad hoc" assumption that $\bar{T}_b = \bar{w} = 1$ was made.^{3,8} In order to solve the multispecies conservation equations, it is necessary to assume that $\bar{T}_b = \bar{w}_i = 1$ and, further, to make an assumption concerning the terms β_i . The product $\beta_i \rho_i$ is the density of the backscattered molecules of species i colliding with the evaporating surface, therefore $\beta_i = \bar{\rho}_{b_i}$.

In Ref. 3 and in the present multispecies moment equation calculated results, the following ad hoc assumption has been made:

$$\frac{\rho_m}{\rho_n} = \frac{(1 + \beta_m)}{(1 + \beta_n)} \frac{\rho_{s_m}}{\rho_{s_n}} \quad (19)$$

where m and n represent any two carbon species.

III. MONTE CARLO SIMULATION OF THE BOLTZMANN EQUATION

A. HIGHER ORDER METHODS

The overall objective of the work discussed in this report has been to provide an accurate theoretical understanding (model) of the strong nonequilibrium processes occurring in a Knudsen layer. Our particular use of such a model has been, as previously indicated, to "back-out" carbon vapor pressure and vaporization kinetics information by applying it to the analysis of carbon laser ablation data.^{2,3} Because the moment equation model (discussed in Section II and previously used for data reduction) requires ad hoc assumptions to solve the conservation equations across a Knudsen layer, a "higher order" solution is needed to eliminate these assumptions and provide the detailed and unique theoretical understanding desired.

It is instructive to think of the classical flows for which higher order simulation methods have been developed. In general, such methods are required whenever the scale lengths of the gradients of density, velocity, pressure, and temperature within a flow become the same order as the mean free path of the molecules. If we define such a scale length by L and the mean free path by λ , then whenever the Knudsen number $Kn = \lambda/L$ becomes greater than about 0.1, a higher order method is needed. In rarefied gas dynamics, λ becomes very large; in a shock wave, L is very small. Both of these flows require modeling on the microscopic (molecular) level. For the Knudsen layer, the need for a higher order model arises both from the magnitude of the gradients of macroscopic variables across the layer and the nonequilibrium boundary conditions at the vaporizing surface.

The Boltzmann equation and the method of Molecular Dynamics have both been extensively used whenever a molecular simulation method is required.^{11,12} In Subsection III-B below, the direct simulation Monte Carlo Method developed by G.A. Bird¹¹ for obtaining solutions to the Boltzmann equation is described. Then, in Subsection III-C, the application of the method to the Knudsen layer problem is discussed. A description of the Molecular Dynamics Method and application to the Knudsen layer problem are discussed in Section IV.

B. DESCRIPTION OF MONTE CARLO/BOLTZMANN EQUATION SIMULATION METHOD

The Monte Carlo method developed by Bird¹¹ can be very effectively used to solve the Boltzmann equation describing the relaxation of nonequilibrium states within a Knudsen layer. The method uses a large number of representative molecules distributed over a number of spatial cells which define the computational domain in physical space. The particle trajectories are found for small time intervals by integrating the Newtonian equations of motion and assigning new position coordinates to each molecule. New molecules are introduced at prescribed inflow boundaries, and appropriate action is taken whenever a molecule encounters a reflecting boundary or leaves the computational domain.

The trajectory increments are followed by molecular indexing and calculation of all molecular collisions which should occur in the prescribed time interval. Possible collision pairs are randomly selected from the simulation molecules within a cell and are accepted or rejected with a known probability of collision. Post-collision velocity components are determined from binary collision dynamics for a prescribed intermolecular potential, generally hard spheres. The above procedures are summarized in the simplified computational flow chart shown in Fig. 2.

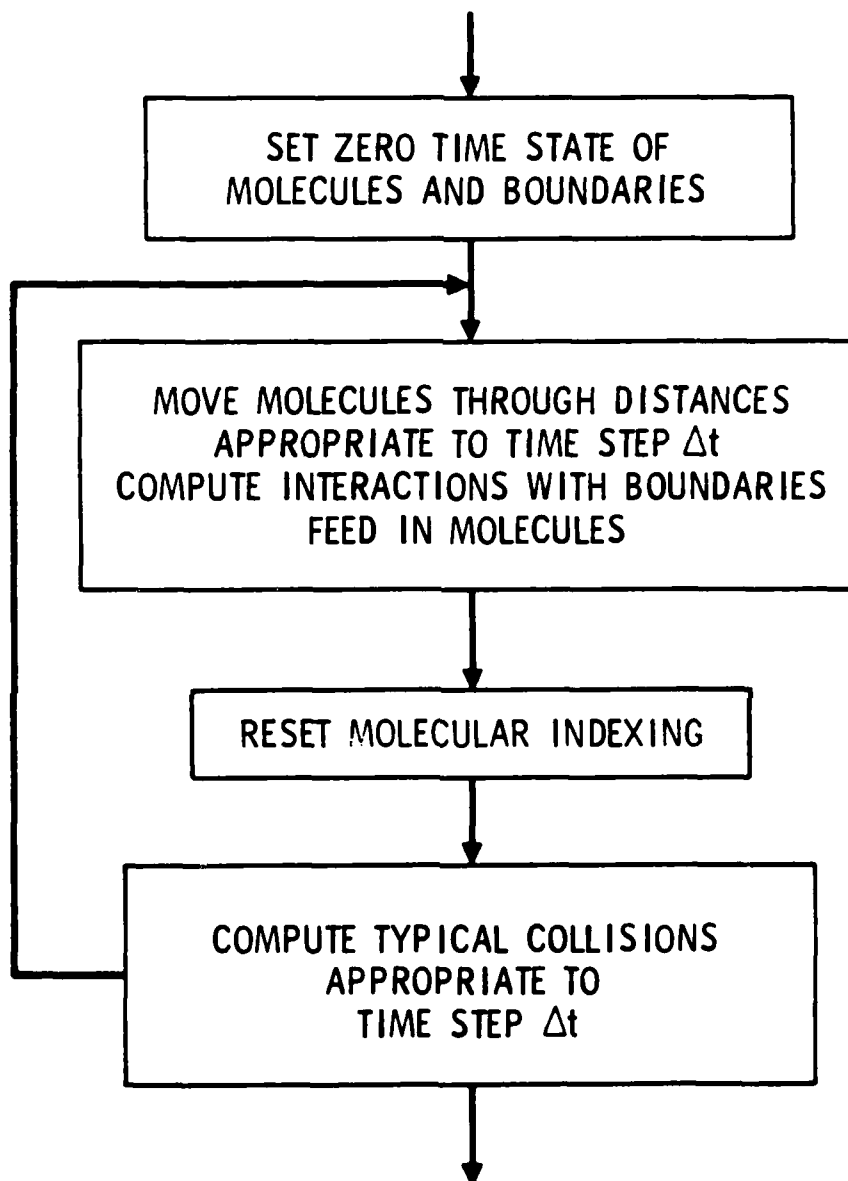


Fig. 2. Main Computational Procedures of the Direct Simulation Monte Carlo Method

Molecular properties, such as mean velocity, number within a cell, temperature, et cetera, are periodically sampled within each cell and retained for time averaging after a statistically steady state has been reached. Averaging usually takes place over a few thousand time increments to reduce the variance of macroscopic properties to an acceptable level. Calculations are always time-dependent, but steady boundary conditions will lead to a statistically steady state in roughly a few molecular transit times through the spatial domain.

These procedures apply for virtually any problem to which the Monte Carlo method can be effectively applied. In the present case, interest lies in the macroscopically one-dimensional problem of outgassing (evaporation) at a prescribed rate from a surface at known temperature. The objective is to determine how flow variables relax through the Knudsen layer to achieve an initially unknown and uniform thermodynamic equilibrium state several mean-free paths from the molecular source.

C. APPLICATION TO THE KNUDSEN LAYER

1. Computer Program Development

A one-dimensional Monte Carlo computer program was written to solve the evaporating Knudsen layer problem. The code has a multi-component and translation-rotation energy exchange capability. Two separate versions were developed. The first treats molecular collisions in the usual three-dimensional physical space. The second employs a two-dimensional physical space for collisions and is intended to provide results which can be directly compared with those from the Molecular Dynamics simulations.

The basic problem of interest prescribes the mass efflux from a surface using the relation

$$\dot{m}_s = \rho_s (RT_s / 2\pi)^{1/2} \quad (20)$$

where ρ_g is a known density of the vaporizing material, T_g is a known surface temperature, R is the gas constant, and \dot{m}_g is the mass flux. This relation, with an appropriately defined density, applies whether the simulation is in two- or three-dimensional physical space.

Molecules leave the surface with a normal velocity selected from the distribution function (normalized so that $\hat{f}_{\max} = 1$)

$$\hat{f}_{u_n} = \sqrt{2\beta} u_n \exp\left(\frac{1}{2} - \beta^2 u_n^2\right); 0 \leq u_n < \infty \quad (21)$$

where $\beta^{-1} = (2RT)^{1/2}$. Velocity components parallel to the wall conform to the distribution function given by

$$\hat{f}_{u_p} = \exp(-\beta^2 u_p^2); -\infty < u_p < \infty \quad (22)$$

In the three-dimensional physical space there are two orthogonal parallel components, and the velocities are selected from a distribution function written in a simplified form. For two-dimensional physical space there is a single parallel component and Eq. (22) is used directly. Eq. (21) applies in either case. The above equations completely specify the source boundary conditions for the Monte Carlo simulations of the Knudsen layer. The scaling of solutions for different types of source boundary conditions is discussed in Appendix A.

2. Downstream Boundary Condition

The downstream boundary condition presents somewhat of a problem because the distribution function cannot be fully determined. Usually, all that can be known is one macroscopic property, such as pressure, temperature, or Mach number and the condition of the thermodynamic equilibrium. Furthermore, these conditions are generally attributed to a so-called "flat sink" that extends to infinity.

The numerical simulation requires a downstream boundary at a finite distance from the source. It is usually possible, however, to locate the downstream boundary so that conditions in the Knudsen layer adjacent to the source are independent of its precise position. It is more difficult to simulate the "flat sink" in the vicinity of the downstream boundary. Cong and Bird¹¹, for example, used a prescribed fractional reflection of molecules incident on the downstream boundary and found that a second (and undesirable) Knudsen layer was formed there. Consequently, they did not successfully simulate the "flat sink" in a strict sense but did find a uniform equilibrium flow between the Knudsen layers.

3. Simulation of the "Flat Sink" Boundary Condition

In the present work, the fractional reflection condition used by Cong and Bird has been adopted, but the downstream cell structure and simulation parameters have been chosen to more closely simulate the "flat sink." This has been achieved in the following way. Since the "flat sink" is in a uniform, steady flow at thermodynamic equilibrium, it is possible to relax conditions generally placed upon cell size and time step. In particular, it appears that these parameters can be selected quite arbitrarily, in principle, without regard to local values of mean-free path and collision frequency. Certain guidelines are obvious: (a) the cell adjacent to the downstream boundary should be much larger than any Knudsen layer that would form there, (b) the number of molecules in the cell should be much larger than the number reflected at the downstream boundary during a single time step, and (c) the time step in the downstream cell should be large enough to establish equilibrium conditions during the collision phase of the computations, yet small enough so that all reflected molecules remain in the cell during the streaming phase.

In the present case, it is possible to choose the downstream cell size, weight factor, and time step so that all these guidelines are easily satisfied. All of the calculations presented herein have placed the downstream boundary at 200 source mean-free paths. The "flat-sink" cell extends from 100 to 200 mean-free paths and the region from the source to 100

mean-free paths was partitioned into 200 cells of equal size. This gives a spatial resolution of 0.5 source mean-free paths per cell in the Knudsen layer region. The actual resolution is somewhat better than this because local free-paths are greater than the source value. The cell grid used is shown schematically in Fig. 3.

4. Calculation Time Steps and Collision Dynamics

The time step in the small cells was less than one-half of the reference collision time and also significantly less than the mean transit time for a cell. The time step for the "flat-sink" was significantly less than the mean transit time yet larger than the mean time between collisions and led to about 3 to 4 collisions per molecule on the average. This was considered long enough to essentially equilibrate the reflected molecules with the others occupying the cell. The small cells contained an average of slightly more than 30 simulated molecules per cell, while the large downstream cell contained approximately 150.

All the calculations used hard-sphere collision dynamics and no internal degrees of freedom. Results were obtained for molecular collisions occurring in both two- and three-dimensional physical space. Table 1 summarizes the principal differences between the parameters of the collision dynamics for simulations in these spaces. The angular functions $F(\theta)$ and $F(\phi)$ refer to the cumulative distributions for scattering angles in a hard-sphere collision.

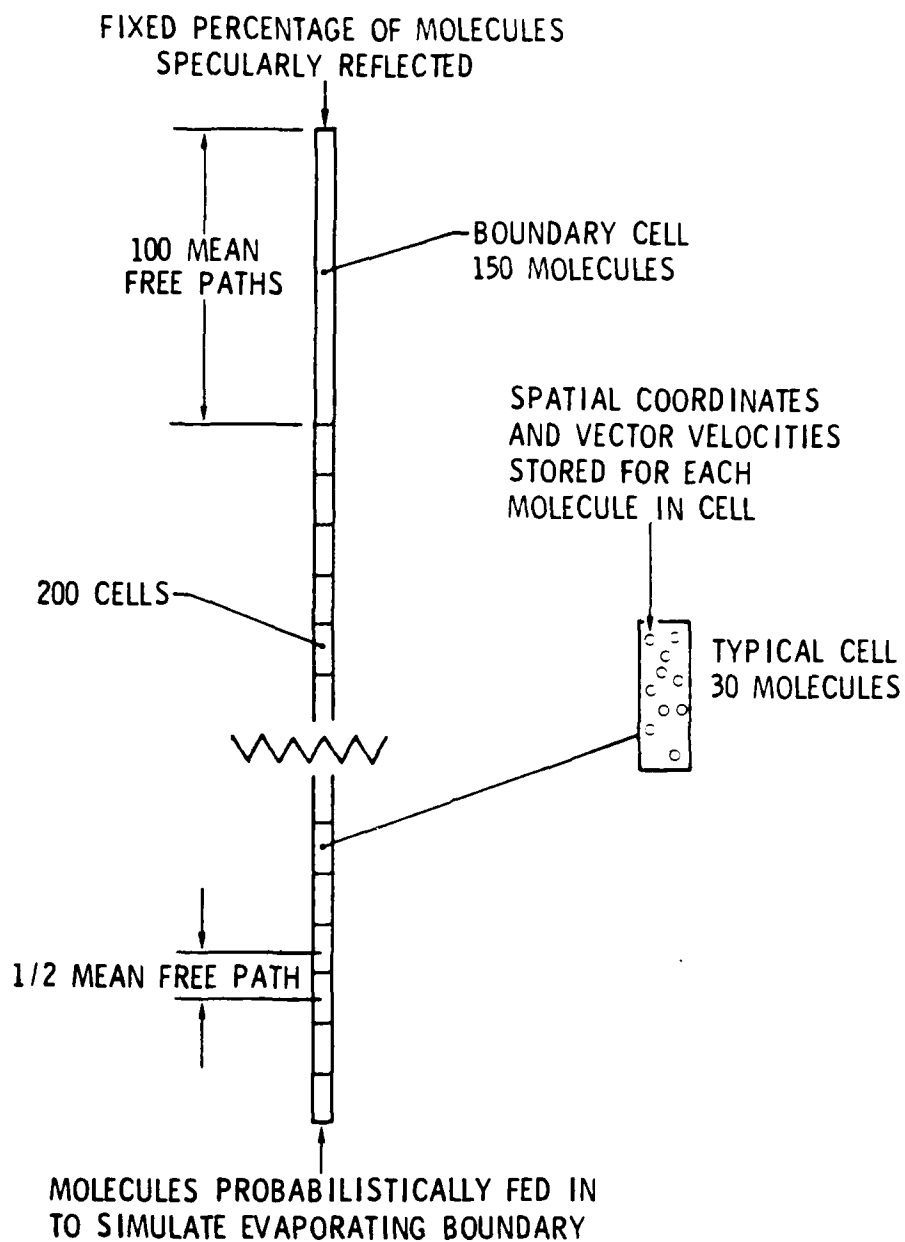


Fig. 3. Cell Grid for Knudsen Layer Simulation

Table 1. Collision Dynamics Parameters

QUANTITY	SYMBOL	3-D SPACE	2-D SPACE
Most Probable Molecular Thermal Speed	$\beta c'_m$	1	$1/2^{1/2}$
Root Mean Square Thermal Speed	$\beta c'_s$	$(3/2)^{1/2}$	1
Average Thermal Speed	$\beta \overline{c}$	$2/\pi^{1/2}$	$\pi^{1/2}/2$
Mean Relative Speed	$\beta \overline{c}_r$	$2^{3/2}/\pi^{1/2}$	$(\pi/2)^{1/2}$
Number Flux	$N/n\overline{c}$	1/4	1/ π
Collision Cross Section	σ	πd^2	2d
Mean Free Path	$\lambda_s \sigma n_s$	$2^{-1/2}$	$2^{-1/2}$
Collision Frequency	$v_s \lambda_s / \overline{c}$	4	π
Pressure	P/nkT	1	1
Translational Temperature	kT	$m\overline{c'^2}/3$	$m\overline{c'^2}/2$
Ratio of Specific Heats for a Monatomic Gas	γ	5/3	2
Cumulative Distribution for Scattering Angle θ	$F(\theta)$	$1/2 [1 - \cos\theta]$ $0 \leq \theta \leq \pi$	$1/2 [1 - \cos(\theta/2)]$ $0 \leq \theta \leq 2\pi$
Cumulative Distribution for Scattering Angle ϕ	$F(\phi)$	$\phi/2\pi$ $0 \leq \phi \leq 2\pi$	N.A.
NOTE: $\beta^{-1} = (2 RT)^{1/2}$			

IV. MOLECULAR DYNAMICS SIMULATIONS

A. DESCRIPTION OF METHOD

The name "Molecular Dynamics Method" is usually associated with the calculation procedure introduced by Alder and Wainwright.¹⁴ It involves the detailed study of the microscopic dynamics of a physical system. Simultaneous trajectories of simulated molecules within a region of physical space are followed in time by integrating the equations of motion for all particles which interact through an assumed intermolecular force field.^{15,16} The method has been applied primarily to the study of dense fluids where many-body collisions are typical. For the study of dilute gases where almost all collisions are binary, the computational efficiency is greatly improved by simplifying the intermolecular force law. For some applications, it has been found that a simple "hard-sphere" model of molecular collisions is sufficient to give meaningful results. In this case, all particles travel in straight-line trajectories between isolated binary collisions.

Molecular Dynamics is a completely deterministic calculation method. By this, it is meant that the spatial location and vector velocities for all particles are known at all times. Particle collisions take place when the centers of two particles come within a molecular diameter of each other. The collision dynamics are then calculated according to the classical hard-sphere model, and the precollision velocity components are replaced by post-collision values.

¹⁴Alder, G.J. and T.E. Wainwright, J. Chem. Phys., 31, 1959, p. 459.

¹⁵Turner, J.S., "From Microphysics to Macrochemistry via Discrete Simulations," Computer Modeling of Matter, ACS Symposium Series No. 86, American Chemical Society, Washington, D.C., P. Lykos (ed.), pp. 231-264.

¹⁶Turner, J.S., "Discrete Simulation Methods for Chemical Kinetics," J. Phys. Chem., 81, 1977, pp. 2379-2408.

This is in contrast to the Monte Carlo/Boltzmann equation calculation method discussed in Section III in which the molecular collisions are calculated probabilistically. That is, the spatial location and vector velocities for all particles are again stored in the computer memory. However, the molecular collisions are calculated by randomly selecting potential collision pairs in a computation cell. The number of collisions per cell per computation time step is determined from the probabilistic form of the collision integral in the Boltzmann equation.¹¹ In this way the exact "deterministic" particle trajectories are replaced by "probabilistic" ones.

B. APPLICATION TO THE KNUDSEN LAYER PROBLEM

The great majority of Molecular Dynamics calculation methods applications has been to isolated or closed systems. The calculations are also usually confined to equilibrium or near equilibrium states.¹⁷ By applying the method to the calculation of the microscopic dynamics of a Knudsen layer, we are considering an open system and a highly nonequilibrium process. In the following, the computational techniques developed for meeting these requirements are described.

Unfortunately, the Molecular Dynamics method is severely restricted by the magnitude of the computing task. For each particle considered, all other particles must be considered as potential collision partners. This leads to the obvious simplification of restricting the collisions to occur two-dimensionally in a plane instead of three-dimensionally in a volume element. This simplification was adopted for our Knudsen layer calculations.

¹⁷Cicotti, G. and A. Tenenbaum, "Canonical Ensemble and Nonequilibrium States by Molecular Dynamics," J. Stat. Phys., 23(6), 1980, pp. 767-772.

In addition to developing techniques to improve the computational efficiency, it was necessary to develop a consistent procedure for introducing particles into the system and allowing them to exit. To do this, the three-area method was developed. This is shown schematically in Fig. 4. Area 1 is effectively a feed cell, while area 3 is a boundary cell. Area 2 is the region simulating the Knudsen layer. Hard sphere particle dynamics are used to calculate particle trajectories in all three areas. Areas 1 and 3 are equilibrium regions at temperatures T_1 and T_3 , respectively. The T_1 is required to be greater than T_3 .

The boundary conditions for areas 1 and 3 are completely periodic, as shown in Fig. 5. Particles leaving any of the boundary surfaces are replaced immediately at the opposite boundary. In this way, all particles leaving immediately reenter with the same velocity components they had upon leaving. The number of particles in areas 1 and 3 is therefore constant, and their velocity distribution is Maxwellian for temperatures T_1 and T_3 , respectively.

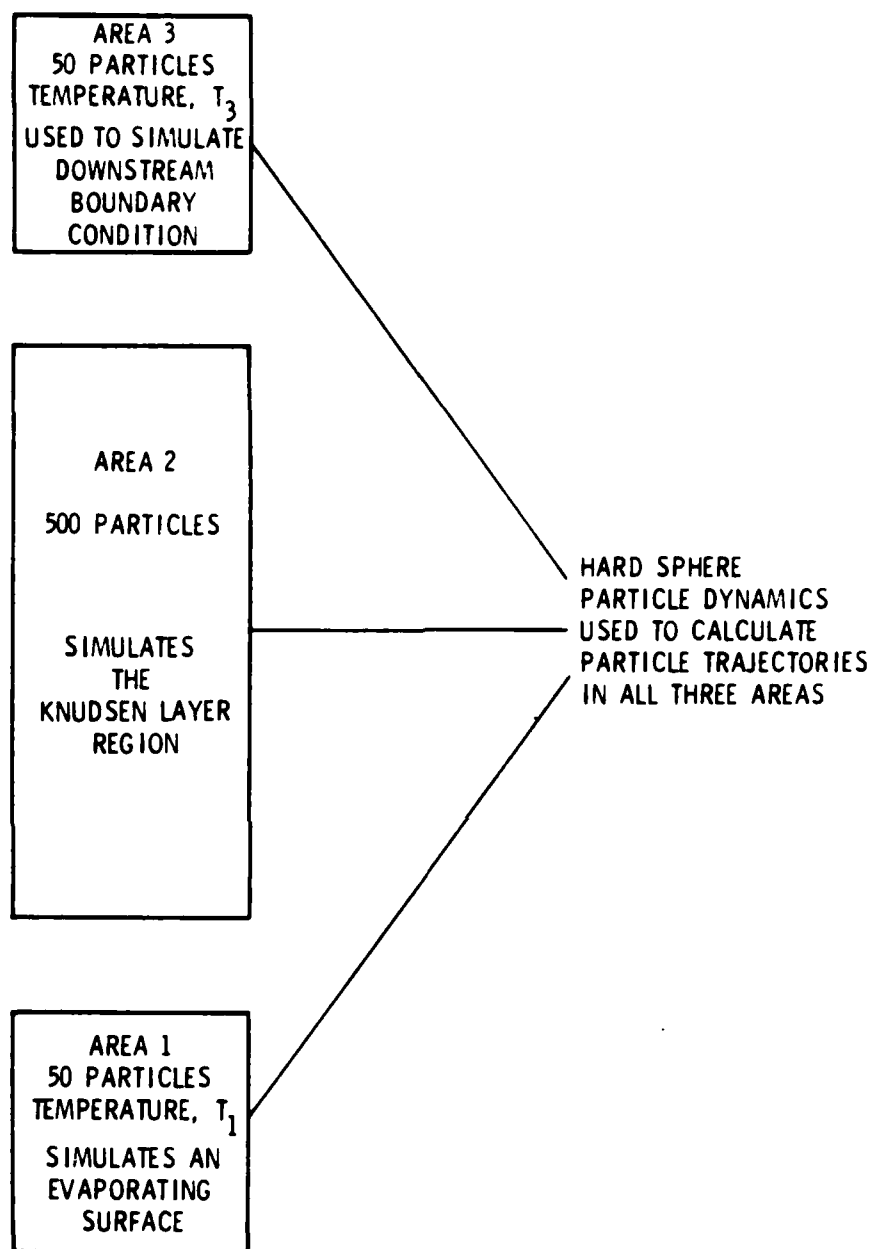


Fig. 4. The Three Area Method

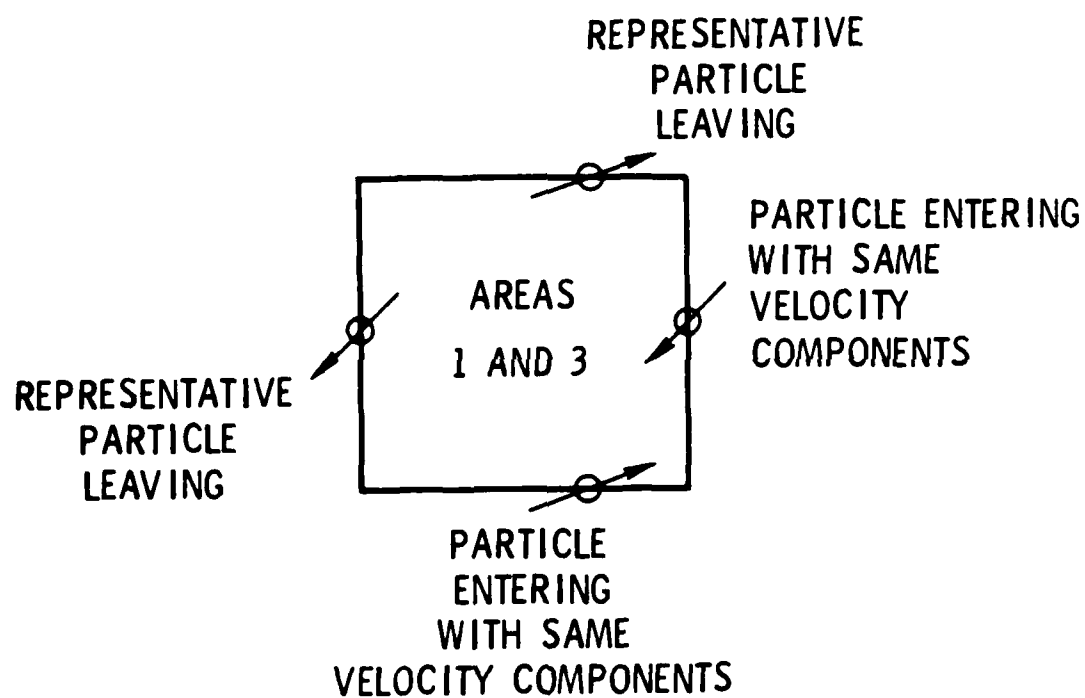


Fig. 5. Periodic Boundary Conditions for Areas 1 and 3

For area 2, the boundary conditions are handled in a manner which simulates the Knudsen layer problem as shown in Fig. 6. The right-hand and left-hand boundaries are again considered to be "periodic." Area 1, below area 2, simulates an evaporating surface by acting as a feed cell. Each time a molecule leaves the upper surface of area 1, a particle having the same physical location and velocity components is introduced upward into area 2. Similarly, each time a particle leaves the lower surface of area 3, a particle having the same velocity components and physical location is introduced downward into region 2 with one modification. Area 3 represents the downstream boundary of the Knudsen layer. At steady state, a mean velocity exists at this boundary. Thus, the particle leaving the lower boundary of area 3 results in the introduction of an identical particle into region 2 only if it has a negative velocity component in the axial direction greater than the mean velocity of molecules leaving the upper boundary of area 2. The particles leaving the upper and lower boundaries of area 2 are deleted from the system (annihilated). Beginning with 300 particles in area 2, in a typical run the number of particles increases to about 475 after 50,000 collisions and then fluctuates between 460 and 490 up to 500,000 collisions as shown in Fig. 7.

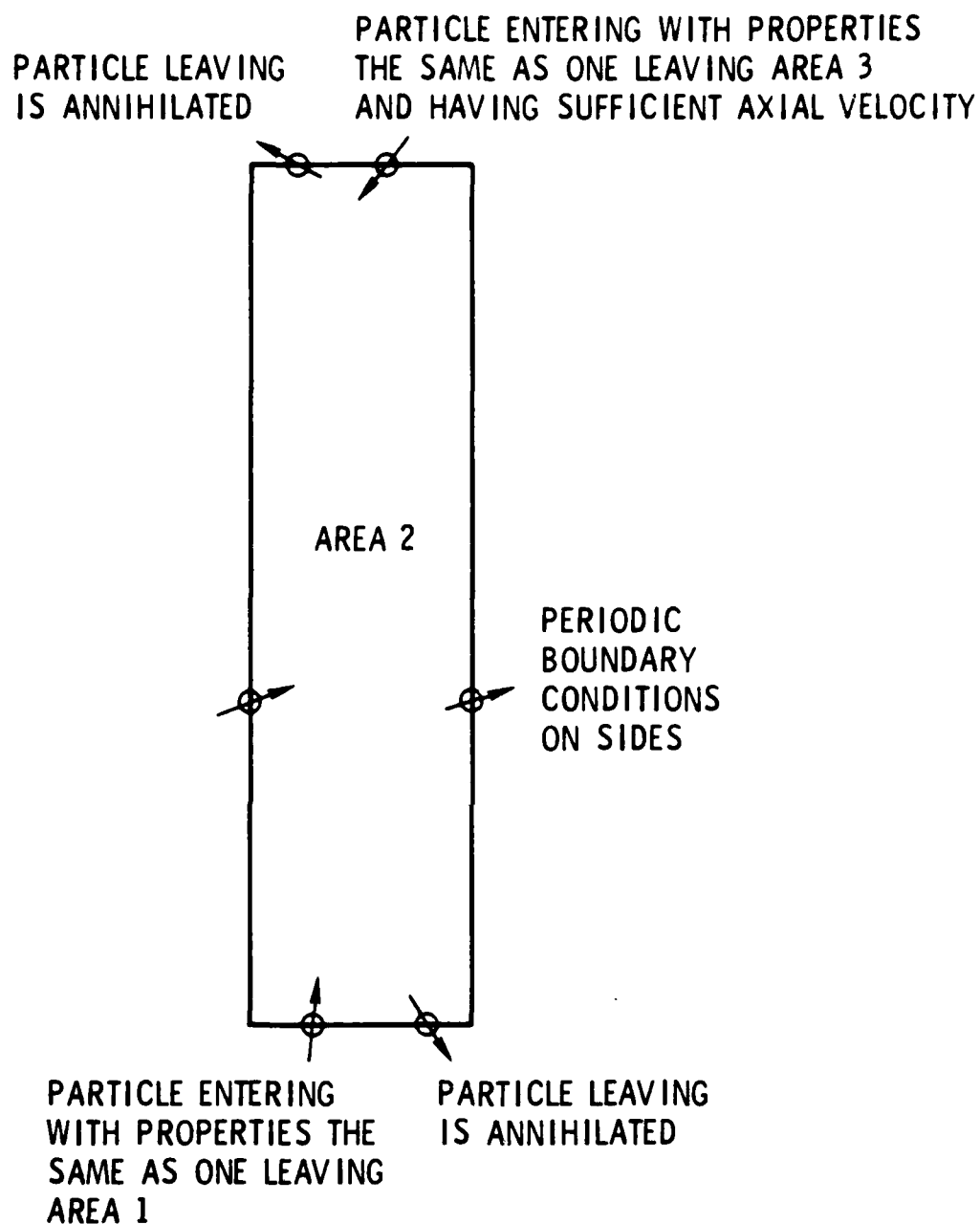


Fig. 6. Boundary Conditions for Area 2
Simulating the Knudsen Layer

NUMBER OF ATOMS vs TIME

AVERAGE MEAN FREE PATH = $6.76\text{E-}08$ m BIN LENGTH = $1.20\text{E-}06$ m

TOTAL TIME = $3.08\text{E-}08$ m ATOMIC RADIUS = $4.00\text{E-}09$ m

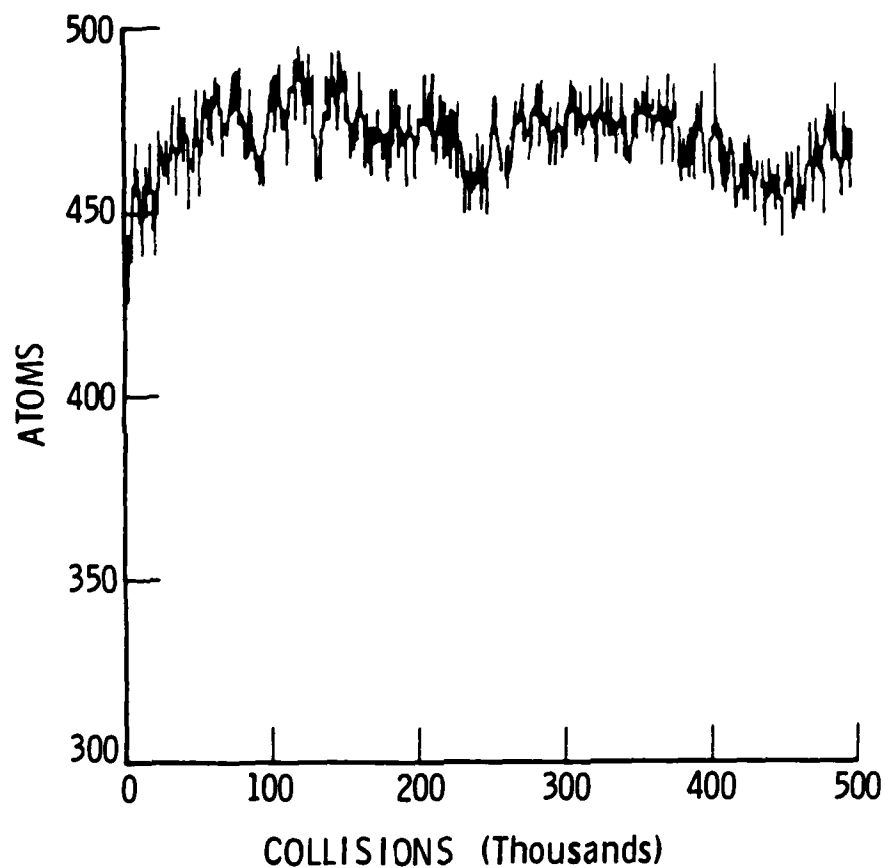


Fig. 7. Number of Particles in Area 2
versus Number of Collisions

V. COMPARISON OF CALCULATED RESULTS

This section will compare Knudsen layer solutions obtained from the moment equation approach (Section II) with those obtained using the higher order solution methods discussed in Sections III and IV. It should be kept in mind that the end objective of these comparisons is to verify that the moment solutions, which we have previously utilized to analyze carbon laser ablation data, are adequate to the extent that carbon vapor pressure and vaporization kinetics conclusions drawn from the data analysis are correct.

The comparisons are presented under three separate headings. In Subsection V-A, the single species moment equation solutions and the single species Monte Carlo/Boltzmann equation solutions are compared. These Knudsen layer solutions are representative of evaporation of substances which vaporize as monatomic species such as aluminum. In Subsection V-B, moment equation solutions and solutions from both higher order methods (Boltzmann equation and Molecular Dynamics) are compared for the simplified case of two-dimensional molecular collisions. This demonstrates modeling capability and (it is hoped) consistency at three levels of mathematical description and establishes a basis for the study of chemical instability phenomena at each of the three levels (see Section VI). Knudsen layer solutions for evaporation of substances which form polyatomic vapor species, such as carbon, are compared in Subsection V-C. To our knowledge, this is the first time that multispecies Boltzmann equation solutions to the Knudsen layer problem have been obtained.

A. SINGLE SPECIES SOLUTIONS, THREE-DIMENSIONAL MOLECULAR COLLISIONS

The four quantities of interest in comparing Knudsen layer solutions obtained by different methods are the mass flux, pressure, density, and temperature ratios across the layer. In the notation described in Section II, these quantities are \dot{m}/m_g , p/p_g , ρ/ρ_g , and T/T_g , respectively. Theoretically, the vapor pressure, p_g , of a substance can be obtained by laser vaporizing it at ambient pressure p , measuring \dot{m} and T_g , and then

employing a Knudsen layer model to supply the quantitative relationships between the measured quantities and the above ratios. We have previously attempted to verify such an approach by obtaining laser vaporization data for a substance for which the vapor pressure at high temperatures is well known.² Unfortunately, experimental difficulties prevented the successful completion of that work. The work described in this report and the comparisons given here seek to establish the validity of the approach analytically.

The first two of the four ratios stated above are the most important for our purposes. Predicted values of these ratios, as a function of the Mach number at the edge of the Knudsen layer, are shown in Fig. 8. The solid lines were obtained from the analytic solutions of the moment equations given in Section II. Also shown are solution values obtained from the Monte Carlo/Boltzmann equation simulations for Knudsen layer edge Mach numbers of 0.58 and 1.0. For further comparison, Table 2 lists the numerical values of all four ratios of interest for both values of edge Mach number.

As illustrated in Fig. 8 and Table 2, the pressure ratio p/p_g predicted by the moment equations is virtually identical to the Boltzmann equation value at $M = 0.58$ and is approximately 1.5 percent low for $M = 1$. Thus, the validity of using pressure ratios p/p_g predicted by the moment equation solutions for obtaining vapor pressure information from laser evaporation data is established. The mass loss ratio \dot{m}/\dot{m}_g also compares very favorably at $M = 0.58$, and the moment equation value is about 2.5 percent lower than the Boltzmann equation value for $M = 1$. This validates the use of mass loss ratios, predicted by the moment equations, for obtaining vaporization kinetics information.

While it is not considered important for the discussion above, the thickness of the Knudsen layer is of interest and will be important for other applications (See Section VI). Density and temperature ratios across the Knudsen layer predicted by the Monte Carlo/Boltzmann equation solutions are shown in Figs. 9 and 10 for Knudsen layer edge Mach numbers of 0.58 and 1.0, respectively. The Knudsen layer thickness increases substantially with increasing Mach number. For $M = 1$, the thickness is about 60 mean free paths. Results similar to these were given previously by Cong and Bird.¹³

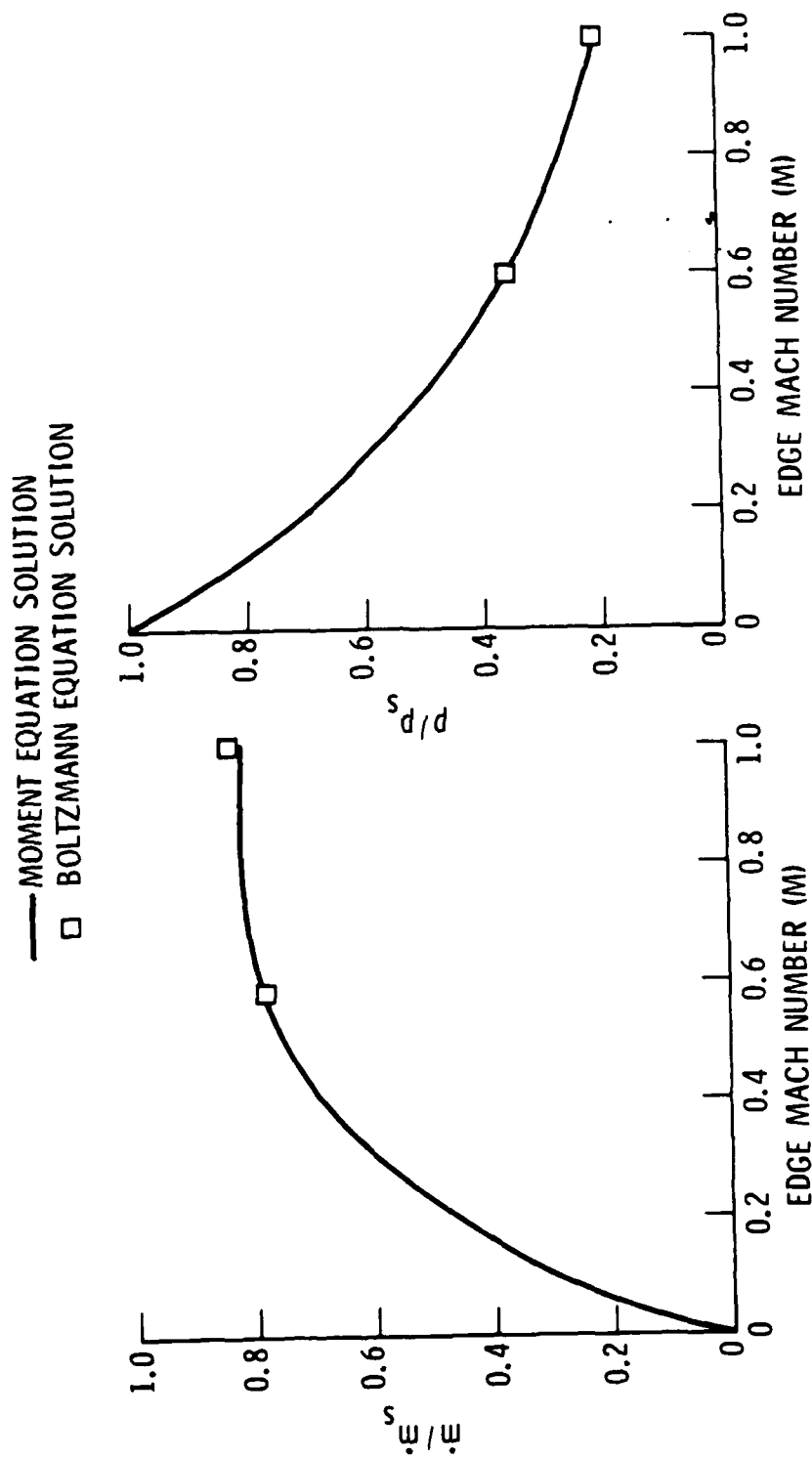


Fig. 8. Comparison of Predicted Mass Loss and Pressure Ratios

Table 2. Predicted Ratios: Single Species

Solution	Edge Mach Number, $M = 0.58$				Edge Mach Number, $M = 1.0$			
	ρ/ρ_s	T/T_s	P/P_s	\dot{m}/\dot{m}_s	ρ/ρ_s	T/T_s	P/P_s	\dot{m}/\dot{m}_s
Moment Equation	0.466	0.791	0.369	0.779	0.306	0.667	0.204	0.815
Boltzmann Equation	0.470	0.785	0.368	0.779	0.324	0.640	0.207	0.837

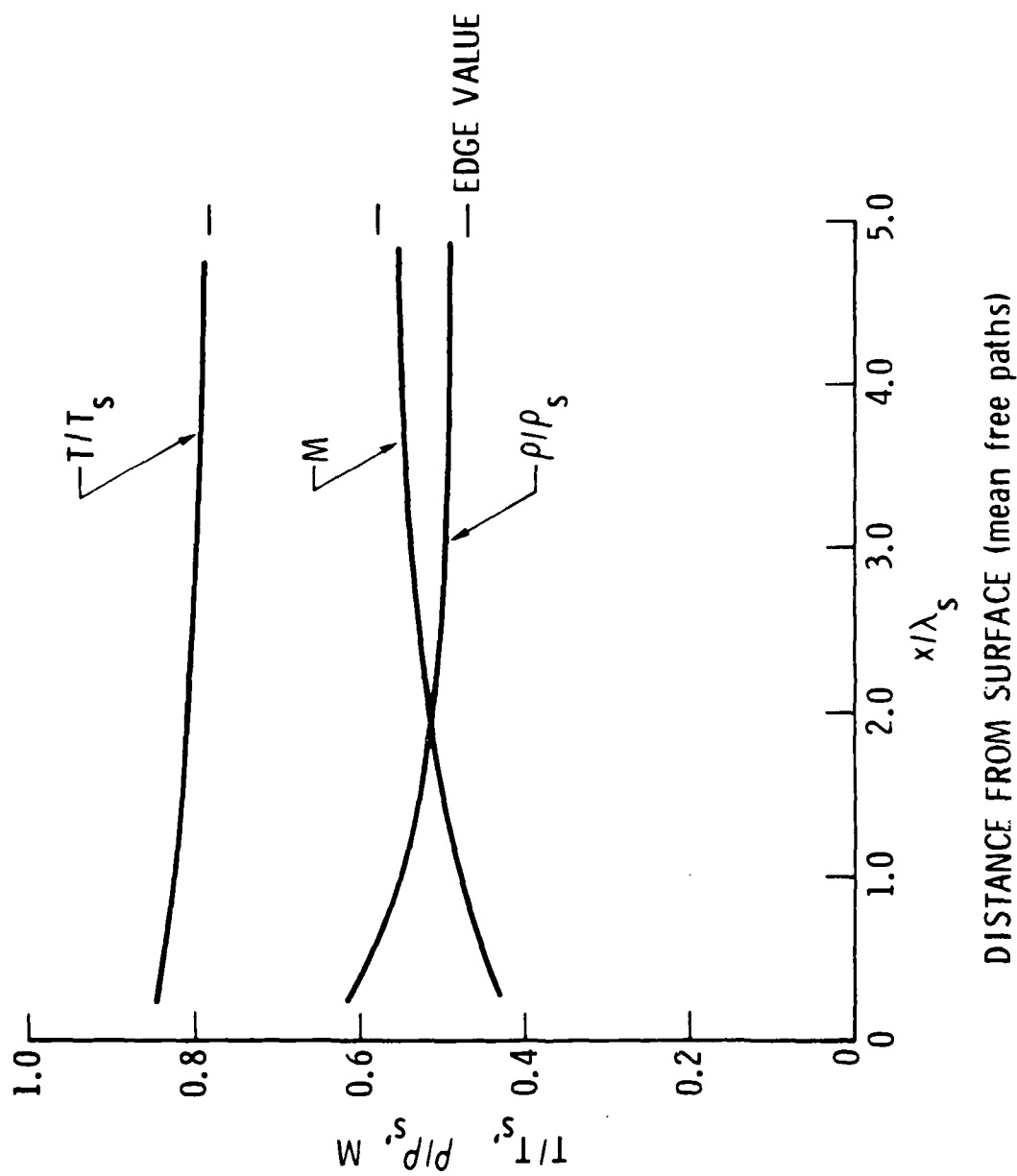


Fig. 9. Knudsen Layer Profiles, $M_{\text{edge}} = 0.58$

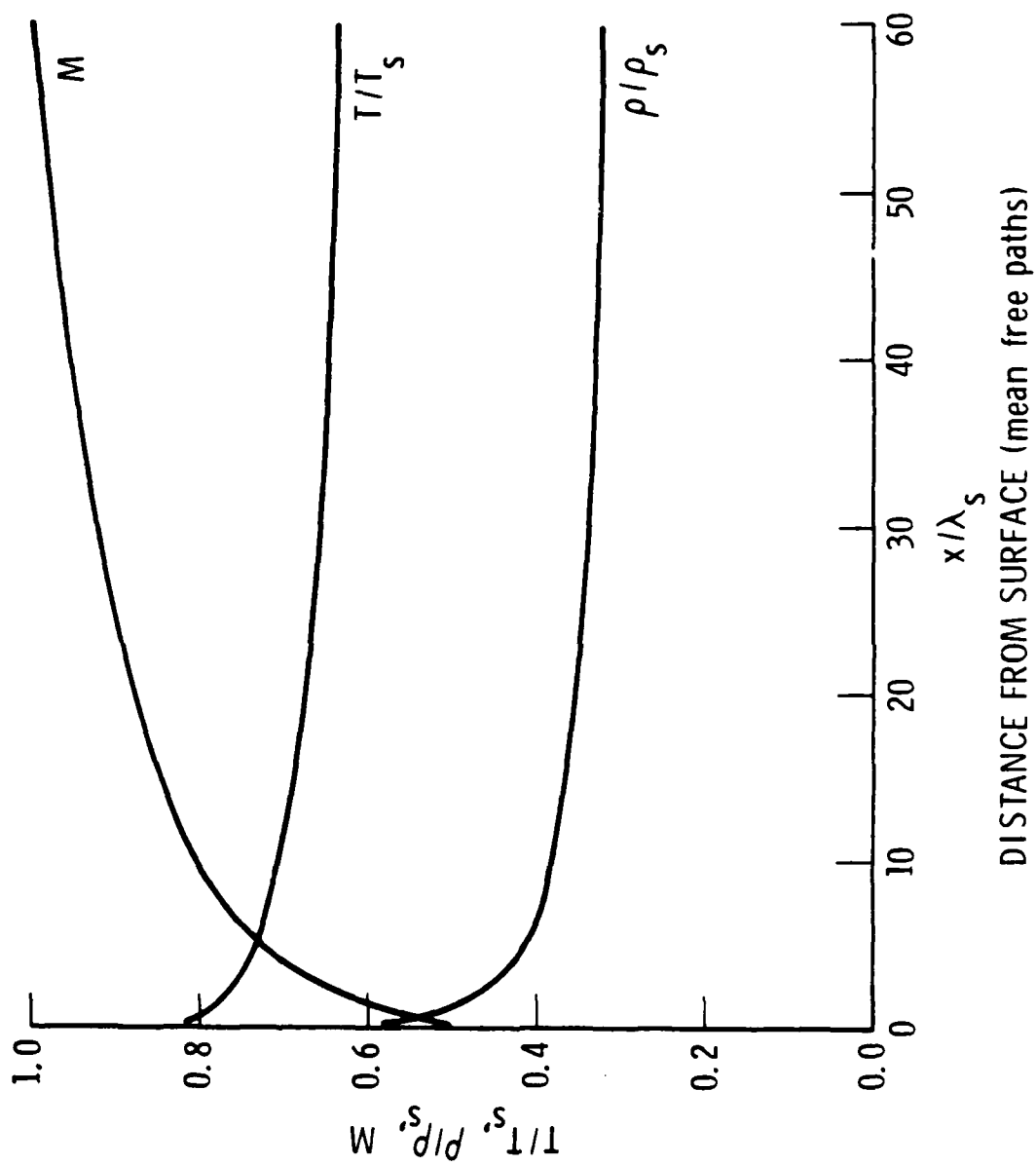


Fig. 10. Knudsen Layer Profiles, $M_{\text{edge}} = 1.0$

B. SINGLE SPECIES SOLUTIONS, TWO-DIMENSIONAL MOLECULAR COLLISIONS

The purpose of this subsection is to compare calculated results obtained from three levels of mathematical complexity, i.e., moment equations, the Boltzmann equation, and Molecular Dynamics. As previously indicated, the comparison of all three methods with one another is limited to solutions obtained for the case of two-dimensional molecular collisions. This is mainly due to computational efficiency requirements for the Molecular Dynamics simulations.

Point-solutions for Knudsen layer edge Mach numbers of 0.53 and 1.0, obtained from Monte Carlo simulations of the Boltzmann equation, are compared with the continuous solutions obtained from the moment equations (Section II) in Fig. 11. The agreement is seen to be very good, especially for the pressure ratios. A single point-solution obtained from the Molecular Dynamics calculations, for an edge Mach number of 0.51, also showed good agreement of the density ratio with the moment equation solution.¹⁸

It is of interest to compare the numerical values of the Knudsen layer solutions for two-dimensional molecular collisions with those obtained for three-dimensional molecular collisions. Such a comparison of moment equation solutions is shown in Fig. 12. For two-dimensional collisions, the mass loss ratio reaches a value about 5 percent higher than that for three-dimensional molecular collisions. Similarly, the pressure and temperature ratios for the two-dimensional case become as much as 15 percent lower than those for the three-dimensional case.

¹⁸Turner, J.S., "Laser-Induced Phase Changes at Solid Surfaces," Final Report, The University of Texas at Austin, October, 1982.

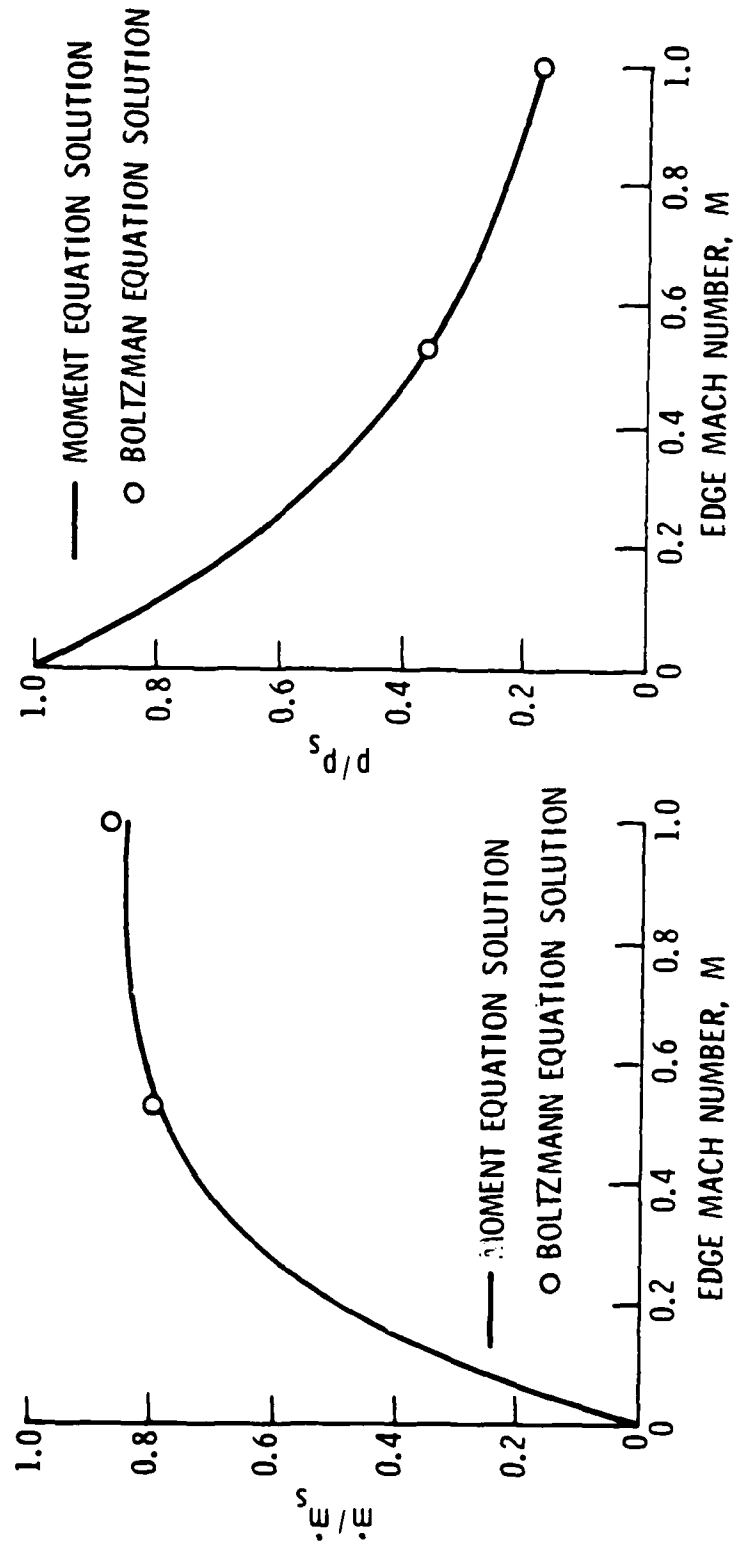
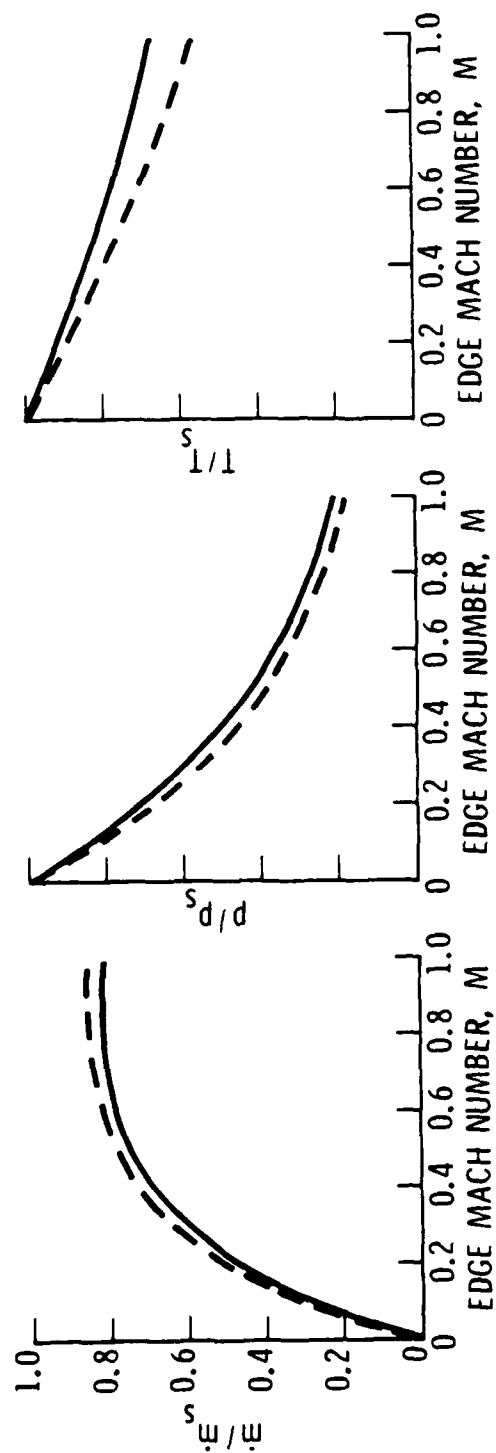


Fig. 11. Comparison of Calculated Results Obtained from Different Solution Methods



MOLECULAR COLLISIONS: SOLID LINE — THREE-DIMENSIONAL
DASHED LINE -- TWO-DIMENSIONAL

Fig. 12. Moment Equation Solutions for Knudsen Layer Jump Conditions

A final comparison of solutions for two-dimensional molecular collisions, obtained by different methods, is shown in Fig. 13. Solutions calculated using Bird's¹¹ moment equation approach are compared with point solutions obtained from the Boltzmann equation. Again the comparison is seen to be very good. Also shown are solutions for three-dimensional collisions.

The comparisons made above further establish the general validity of the moment equation approach, one of the principle objectives of this work. In addition, a computational framework has been established to allow baseline solutions for more complex problems involving nonlinear chemical reactions to be obtained. It is anticipated that problems of this type will demonstrate the greatest utility of the Boltzmann equation and Molecular Dynamics solution methods (see Section VI).

C. MULTISPECIES SOLUTIONS

The multispecies moment equation solutions discussed in Subsection II-C predict the change in temperature, pressure, and species concentration across the Knudsen layer as a function of edge Mach number. Comparison of results calculated from these equations with those predicted by a Monte Carlo simulation of the multispecies Boltzmann equation are discussed below. These solutions correspond most closely to the polyatomic carbon evaporation (sublimation) process which we are seeking to understand. The only difference between the Monte Carlo simulated results discussed herein and the moment equation solutions used for carbon laser ablation data reduction in Ref. 3 is that the latter contained additional terms allowing for the internal degrees of freedom of the polyatomic carbon species. It was considered most important to examine the validity of the ad hoc closure procedure without the internal degrees of freedom.

For the multispecies moment equations, additional ad hoc closure assumptions [i.e., Eq. (19)] are needed. Some indication of the importance of these arbitrary assumptions is indicated by comparing moment equation and

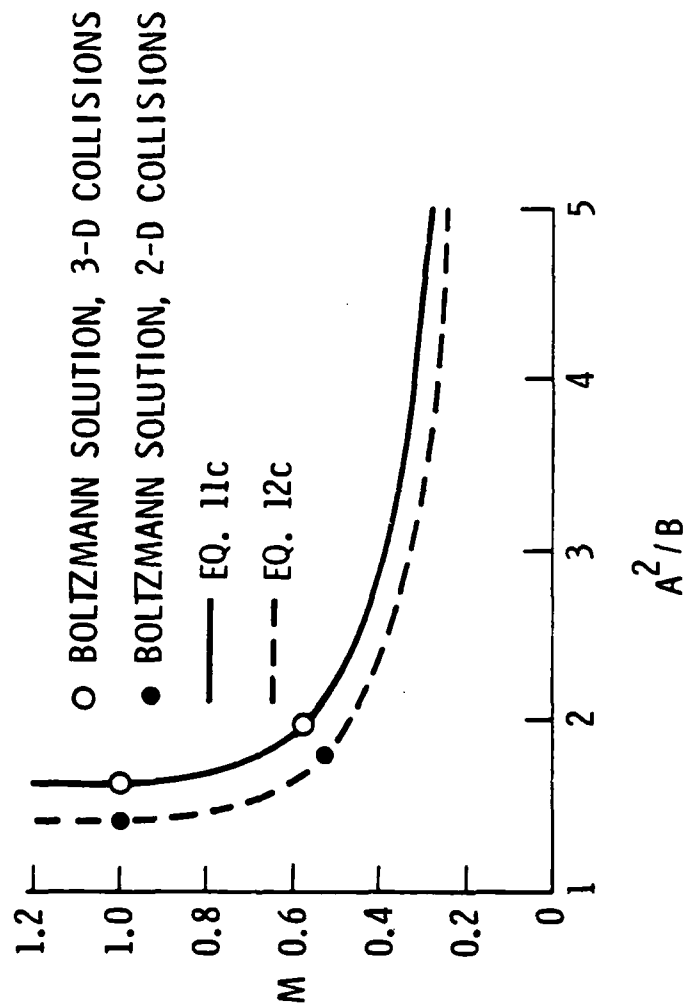


Fig. 13. Parameter A^2/B as a Function of Knudsen Layer Edge Mach Number

Boltzmann equation predicted ratios of microscopic variables. This is shown in Table 3 as are the single species moment equation and Boltzmann equation predicted values. From this, two observations can be made. For the multispecies calculations, the approximate solutions are reasonably good (within 5 percent). Further, the multispecies results are very close to the single species results. Details of the species distributions predicted by the two calculation methods are shown in Table 4. For both density ratios (mass fractions) and pressure ratios (mole fractions), the trends in agreement and disagreement are similar. For the dominant species C_3 , the approximate and Boltzmann equation calculated results agree within 1 percent. For the lighter species C_1 and C_2 , the density and pressure ratios predicted by the moment equations are up to 7 percent high, whereas for the heavier species C_4 and C_5 the predicted ratios are up to 12 percent low. We intend to further investigate other uses for the Boltzmann equation solutions that could improve the ad hoc assumptions, i.e., Eq. (19).

The good agreement of the approximate and more exact solutions for the dominant C_3 species and the reasonable agreement for the other species indicate that our carbon vapor pressure and vaporization kinetics conclusions in earlier work,³ based upon the moment equation solutions, are correct within experimental accuracies.

Table 3. Predicted Ratios of Macroscopic Variables

Solution	Edge Mach Number, $M = 0.58$				Edge Mach Number, $M = 1.0$			
	ρ/ρ_g	T/T_g	p/p_g	\dot{m}/\dot{m}_g	ρ/ρ_g	T/T_g	p/p_g	\dot{m}/\dot{m}_g
Single Species Moment Equation	0.466	0.791	0.369	0.779	0.306	0.667	0.204	0.815
Single Species Boltzmann Equation	0.470	0.785	0.368	0.779	0.324	0.640	0.207	0.837
Multispecies Moment Equation	0.461	0.797	0.372	0.771	0.302	0.677	0.206	0.810
Multispecies Boltzmann Equation	0.451	0.786	0.355	0.770	0.315	0.642	0.202	0.826

Table 4. Predicted Species Distributions

Solution	P_i/P				
	1	2	i=3	4	5
Moment Equation	0.0872	0.146	0.727	0.0127	0.0275
Boltzmann Equation	0.0852	0.136	0.734	0.0129	0.0314

Solution	ρ_i/ρ				
	1	2	i=3	4	5
Moment Equation	3.17×10^{-2}	1.06×10^{-3}	0.793	1.85×10^{-2}	5.00×10^{-2}
Boltzmann Equation	3.09×10^{-2}	9.88×10^{-3}	0.799	1.87×10^{-2}	5.70×10^{-2}

VI. OTHER APPLICATIONS

The Monte Carlo/Boltzmann equation and Molecular Dynamics simulation methods, as applied to the Knudsen layer and discussed in Sections III and IV, have considerable potential for application to many other complex problems of chemistry and physics. These problems are, in general, characterized by the interaction of a large number of individual degrees of freedom. Because of this, the usual conservation equations no longer form a closed set. This leads to great theoretical, and practical, difficulties. For example, when the mean free path becomes large relative to the typical length scale of the gradients of conserved quantities within a flow, the classical Chapman-Enskog theory and the Navier-Stokes equations cease to be valid. Gas dynamic problems of this nature motivated the development of the Monte Carlo/Boltzmann equation simulation method by Bird.^{11,19} Other examples of physical/chemical problems where interaction of a large number of degrees of freedom must be taken into account are nucleation phenomena and chemical instability phenomena.^{15,16}

One possible avenue of new work which we are exploring is the determination of internal state molecular relaxation kinetics. An appropriate probabilistic model for rotational and vibrational relaxation kinetics would be incorporated into our Monte Carlo/Boltzmann equation simulation code. Thermodynamic (i.e., internal state and translational) temperatures would then be spectroscopically "mapped" in the nonequilibrium plume flowfield emanating from a laser vaporized spot. If a slot-focussed laser beam were used, it would be possible to probe an isocollisional volume element in a flowfield with planar symmetry. Such an experiment is shown schematically in Fig. 14. Initial experiments would vaporize substances such as CO_2 or H_2O for which spectroscopic data are well characterized. It is hoped that later experiments could be conducted for the carbon triatomic molecule C_3 . We have recently

¹⁹Bird, G.A., "Monte Carlo Simulation of Gas Flows," Ann. Rev. Fluid Mech., 1978, pp. 11-31.

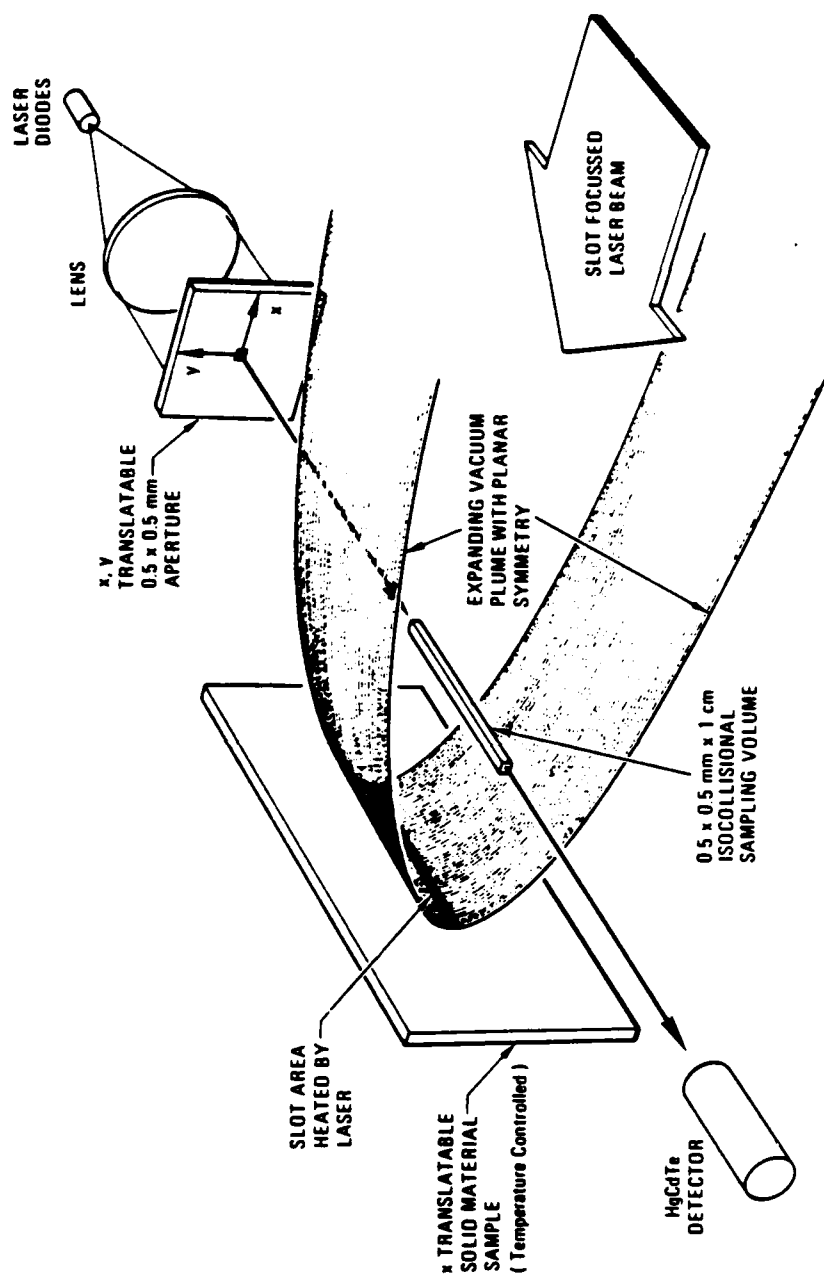


Fig. 14. Thermodynamic Temperature Probe Experiment

proposed initial experiments.²⁰ Kinetic rate data would be obtained by comparing model prediction with the experimental data. The technique is closely related to the work of Levy.²¹

It may be possible to also study chemical relaxation rates by a method similar to the above. It appears desirable to maintain a flow field with planar symmetry through the use of a slot-focussed laser beam. If one reactant species were laser-vaporized into an ambient environment of a second reactant and the product concentration contours were "mapped" spectroscopically in the flow field, the reaction kinetics could be studied by comparing them with predicted results. In some instances it might even be possible to study the effect of reactant internal energy states on the chemical reaction rate. This would be accomplished by first developing an understanding of the internal energy relaxation kinetics of a molecule of interest by the technique discussed in the preceding paragraph. Then, the substance could be laser-vaporized, at a rate appropriate to "prepare" it in a specific internal energy state, and allowed to mix with ambient reactant molecules in a rarefied gas dynamics environment.

A third applications idea, likely to take full advantage of the Reactive Molecular Dynamics method,¹⁶ is the study of the theoretically very difficult problem of the effect of thermal fluctuations in nonlinear chemical systems. The great majority of theoretical work on chemical instability phenomena has been concerned with fluctuations in species concentrations.^{15,22,23} Recently,

²⁰Baker, R.L. and K.C. Herr, "A New Approach for the Study of Translational and Internal State Molecular Relaxation Kinetics," The Aerospace Corporation, Letter Proposal, El Segundo, CA, May 1982.

²¹Levy, D.H., "The Spectroscopy of Very Cold Gases," Science, 214, 16 Oct. 1971, pp. 263-269.

²²Nicolis, G. and I. Prigogine, Self-Organization in Nonequilibrium Systems, John Wiley & Sons, NY, 1977.

²³Glansdorff, P. and I. Prigogine, Thermodynamic Theory of Structure, Stability and Fluctuations, Wiley-Interscience, 1971.

the effect of thermal fluctuations in nonlinear chemical systems has been examined²⁴ using a linearized Knudsen layer model combined with a nonlinear reaction rate term. The objective is to study "extinction" and "ignition" points^{24,25} associated with exothermic reactions in open systems, i.e. explosions. We plan to extend the work of Ref. 24 to include nonlinear Knudsen layer effects through further development of our Monte Carlo/Boltzmann equation and Molecular Dynamics simulation methods. In addition, a promising new method, termed the chemical velocity distribution (CVD) method, has been implemented and validated at the University of Texas for spatially uniform systems.¹⁸ By using a hierarchy of simulation methods, such as these, we can obtain fundamental microscopic information concerning the effect of thermal fluctuations, as well as the coupling of energy release and molecular dynamics phenomena in explosive chemically reacting systems.

²⁴Nicolis, G., F. Baras, and M. Malek Mansour, "Thermal Fluctuations in Nonlinear Chemical Systems," Preprint, Universite' Libre de Bruxelles, Bruxelles, Belgium.

²⁵Kondratiev, N.V. and E.E. Nikitin, Gas-Phase Reactions, Springer, Berlin, 1980.

VII. SUMMARY AND CONCLUSIONS

Motivated by the desire to eliminate ad hoc closure assumptions associated with moment equation solutions, we have obtained higher order solutions to the Knudsen layer problem for strong evaporation. In order to investigate Knudsen layer solutions based upon the consideration of microscopic molecular collision dynamics, two different computer simulation techniques have been used. In the first, Boltzmann equation solutions were obtained by a direct simulation Monte Carlo method. These solutions represent consideration of probabilistic molecular trajectories. In the other simulation method, simplified deterministic molecular trajectories were calculated for a simulated Knudsen layer region using the method of Molecular Dynamics.

In earlier work, we obtained carbon vapor pressure and vaporization kinetics information from laser-vaporized carbon ablation data. To accomplish this, we utilized an approximate Knudsen layer solution based upon the mass, momentum, and energy conservation (moment) equations across the Knudsen layer. Simulated Monte Carlo/Boltzmann equation results, retaining the multispecies character of carbon vapor, have been calculated and compared with results predicted by the simpler moment equation approach. The agreement of the essential features of solutions obtained by the two methods validates the use of the moment equation approach for obtaining the carbon thermochemical properties. This is believed to be the first time that multispecies Boltzmann equation solutions to the Knudsen layer problem have been obtained.

To maintain reasonable computation time efficiency, the Molecular Dynamics simulations of the Knudsen layer were restricted to two-dimensional (planar) molecular collisions and to a single species. Direct comparison of calculated results from all three modeling levels, i.e., moment equations, Boltzmann equation, and Molecular Dynamics, was made possible by extending (restricting) the moment equation and Monte Carlo/Boltzmann equation methods

to the consideration of two-dimensional molecular collisions. The mutual agreement of these calculated results with one another further establishes the validity of the moment equation approach. In addition, a modeling framework has now been laid for application of the computer simulation methods to complex and theoretically difficult physical/chemical problems such as the effect of thermal fluctuations in nonlinear chemical systems.

REFERENCES

1. Knudsen, M., Ann. Phys. (Leipzig), 47, 1915, pp. 697-708.
2. Baker, R.L., "Carbon Nonequilibrium Phase Change," Office of Naval Research Interim Report, TR-0011(6728-02)-1, The Aerospace Corporation, El Segundo, CA, Dec. 1981.
3. Baker, R.L. and M.A. Covington, "The High Temperature Thermochemical Properties of Carbon," Office of Naval Research Interim Report, TR-0082(2729)-1, The Aerospace Corporation, El Segundo, CA, Mar. 1982.
4. Weichert, H., "Boundary Conditions for the Liquid-Vapor Interface of Helium II," J. Phys. C: Solid State Physics, 9, 1976, pp. 553-569.
5. Baker, R.L., "An Irreversible Thermodynamics Model for Graphite Sublimation in Radiation Environments," Progress in Astronautics and Aeronautics: Outer Planet Heating and Thermal Protection Systems, 64, R. Viskanta (ed.), AIAA, New York, 1979, pp. 210-227.
6. Bornhorst, W.J. and G.N. Hatsopoulos, "Analysis of a Phase Change by the Methods of Irreversible Thermodynamics," J. Appl. Mech., 34, Dec. 1967, pp. 840-846.
7. Baker, R.L., "A Multiple Species Nonequilibrium Thermodynamics Model for Carbon Sublimation," J. Nonequil. Thermo., 7(6), 1982, pp. 309-322.
8. Anisimov, S.I., "Vaporization of Metal Absorbing Laser Radiation," Sov. Phys. JETP, 27(1), 1968, pp. 182-183.
9. Ytrehus, T., "Theory and Experiments on Gas Kinetics in Evaporation," Progress in Astronautics and Aeronautics: Rarefied Gas Dynamics, 51 (II), J.L. Potter (ed.), AIAA, New York, 1977, pp. 1197-1212.
10. Knight, C.J., "Theoretical Modeling of Rapid Surface Vaporization with Back-Pressure," AIAA J., 17, May 1979, pp. 519-523.
11. Bird, G.A., Molecular Gas Dynamics, Oxford University Press, London, 1976.
12. Hansen, H.W., and W.C. Schieve, J. Stat. Phys., 3, 1971, p. 35.
13. Cong, T.T. and G.A. Bird, "One-Dimensional Outgassing Problem," Phys. Fluids, 21(3), 1978, pp. 327-333.
14. Alder, G.J. and T.E. Wainwright, J. Chem. Phys., 31, 1959, p. 459.

REFERENCES (Continued)

15. Turner, J.S., "From Microphysics to Macrochemistry via Discrete Simulations," Computer Modeling of Matter, ACS Symposium Series No. 86, American Chemical Society, Washington, D.C., P. Lykos (ed.), pp. 231-264.
16. Turner, J.S., "Discrete Simulation Methods for Chemical Kinetics," J. Phys. Chem., 81, 1977, pp. 2379-2408.
17. Cicotti, G. and A. Tenenbaum, "Canonical Ensemble and Nonequilibrium States by Molecular Dynamics," J. Stat. Phys., 23(6), 1980, pp. 767-772.
18. Turner, J.S., "Laser-Induced Phase Changes at Solid Surfaces," Final Report, The University of Texas at Austin, October 1982.
19. Bird, G.A., "Monte Carlo Simulation of Gas Flows," Ann. Rev. Fluid Mech., 1978, pp. 11-31.
20. Baker, R.L. and K.C. Herr, "A New Approach for the Study of Translational and Internal State Molecular Relaxation Kinetics," The Aerospace Corporation, Letter Proposal, El Segundo, CA, May 1982.
21. Levy, D.H., "The Spectroscopy of Very Cold Gases," Science, 214, 16 Oct. 1971, pp. 263-269.
22. Nicolis, G. and I. Prigogine, Self-Organization in Nonequilibrium Systems, John Wiley & Sons, NY, 1977.
23. Glansdorff, P. and I. Prigogine, Thermodynamic Theory of Structure, Stability and Fluctuations, Wiley-Interscience, 1971.
24. Nicolis, G., F. Baras, and M. Malek Mansour, "Thermal Fluctuations in Nonlinear Chemical Systems," Preprint, Universite' Libre de Bruxelles, Bruxelles, Belgium.
25. Kondratiev, N.V. and E.E. Nikitin, Gas-Phase Reactions, Springer, Berlin, 1980.

APPENDIX A

SOURCE BOUNDARY CONDITIONS

The Knudsen layer solutions for the problems of surface outgassing and surface evaporation are closely related. The purpose of this Appendix is to show how numerical results for the outgassing case can be simply related to equivalent results for the evaporating case. Reference 11 and the Monte Carlo calculated results we have discussed in this report used the outgassing form of the surface boundary condition. The evaporation problem results (tabulated) were obtained using the scaling relationships given below.

The directed mass fluxes away from the surface, designated by the superscript +, are given by

$$\dot{m}_s^+ = \rho_s \sqrt{\frac{RT_s}{2\pi}} \quad (\text{evaporation}) \quad (\text{A-1a})$$

$$\dot{m}_g^+ = \rho_g \sqrt{\frac{RT_s}{2\pi}} \quad (\text{outgassing}) \quad (\text{A-1b})$$

for the evaporation and outgassing problems, respectively. In both cases, the temperature is the saturated vapor temperature T_s . Since we wish to solve the outgassing problem and relate the results to the evaporation problem, the net mass flux \dot{m} and the directed mass flux (backscattered) toward the surface \dot{m}^- must satisfy the following equations.

$$\dot{m} = \dot{m}_s = \dot{m}_g \quad (\text{A-2a})$$

$$\dot{m}^- = \dot{m}_s^- = \dot{m}_g^- \quad (\text{A-2b})$$

The net, positive directed, and negative directed mass fluxes are related by

$$\dot{m} = \alpha_v \dot{m}^+ - \alpha_c \dot{m}^- \quad (\text{A-3a})$$

where α_v is the evaporation coefficient and α_c is the condensation coefficient. For the outgassing problem $\alpha_v = 1.0$ and $\alpha_c = 0$, Eq. (A-3a) thus becomes

$$\dot{m}_g = \dot{m}_g^+ \quad (\text{A-3b})$$

For the evaporation problem $\alpha_v = \alpha_c = 1.0$, and we have

$$\dot{m}_s = \dot{m}_s^+ - \dot{m}_s^- \quad (\text{A-3c})$$

Subtracting Eqs. (A-3b) and (A-3c) and substituting from Eqs. (A-2a) and (A-2b), we obtain

$$\dot{m}_s^+ = \dot{m}_g^+ + \dot{m}_g^- \quad (\text{A-3d})$$

Substituting from Eqs. (A-1a) and (A-1b) and defining $\xi = \dot{m}_g^- / \dot{m}_g^+$, we find that the relationship between ρ_s and ρ_g becomes

$$\frac{\rho_s}{\rho_g} = 1 + \xi \quad (\text{A-4a})$$

Thus, Knudsen layer density jumps ρ/ρ_g calculated for the outgassing problem can be related to ρ/ρ_g for the evaporation problem by

$$\frac{\rho}{\rho_s} = \frac{\rho}{\rho_g} \left[\frac{1}{1+\xi} \right] \quad (\text{A-4b})$$

From the above equations, it can be easily shown that once ξ is determined from the numerical Monte Carlo outgassing solution, the mass flux ratio for the evaporation problem is given by

$$\frac{\dot{m}}{\dot{m}_s} = \frac{1}{1+\xi} \quad (\text{A-5})$$

APPENDIX B

TRANSLATIONAL ENERGY FLUX EQUATION FOR TWO-DIMENSIONAL MOLECULAR COLLISIONS

The moment equation solutions discussed in Section II have considered the cases of both two-dimensional and three-dimensional molecular collisions. The purpose of the present discussion is to briefly show how the differences in the energy conservation equations for the two cases arise in the macroscopic balance equations.

Following the procedure and notation of Bird¹¹, the following equation may be written for the inward flux of a quantity Q across an element of surface area per unit time.

$$\frac{1}{A} \frac{dQ}{dt} = \frac{n\beta^3}{\pi^{3/2}} \int_{-\infty}^{\infty} \int_{-\infty}^{\infty} \int_{-c_0 \cos \theta}^{\infty} Q(u' + c_0 \cos \theta) \exp \left\{ -\beta^2 (u'^2 + v'^2 + w'^2) \right\} du' dv' dw' \quad (B-1)$$

It can be shown that for the mass flux and momentum flux equations, the resulting integrated equations are algebraically the same for the cases of two- and three-dimensional collisions with an appropriately defined density. The translational energy flux equations for the two cases, however, are not the same.

Substituting $Q = \frac{1}{2} m c^2 = \frac{1}{2} m (u^2 + v^2 + w^2)$ and recalling that

$$u = u' + c_0 \cos \theta$$

$$v = v' + c_0 \sin \theta$$

$$w = w'$$

we may integrate Eq. (B-1) to give

$$\frac{\beta^3 q_{i, tr}}{nm} = \left(\frac{1}{4\pi^{1/2}} \right) \left\{ (s^2 + 2) \exp(-s^2 \cos^2 \theta) + \pi^{1/2} s \cos \theta [s^2 + 5/2] [1 + \operatorname{erf}(s \cos \theta)] \right\} \quad (B-2)$$

Equation (B-2) is for three-dimensional molecular collisions. For two-dimensional molecular collisions, $w = w' = 0$ and the integration is performed only over the velocities u' and v' . The result is identical to that given by Eq. (B-2), except that the factors 2 and 5/2 are replaced by 3/2 and 2, respectively.

The outward translational energy flux $q_{0, tr}$ is obtained from Eq. (B-2) simply by setting s equal to zero. The net energy flux is the product of the mass flux ρu and the sum of the internal and kinetic energies. The internal energies for three-dimensional and two-dimensional molecular collisions are $(5/2)RT$ and $2RT$, respectively. This arises because there are three translational degrees of freedom versus two translational degrees of freedom.

When the results are combined for the inward, outward, and net energy fluxes discussed above, the text equations (4a) and (4b) are obtained for three-dimensional and two-dimensional molecular collisions, respectively.

END

FILMED

9-83

DTIC